

AFWL-TR-69-87

AFWL-TR-
69-87

Switching Notes
Note 7

LASER-TRIGGERED SWITCHING STUDY

John J. Moriarty

Ion Physics Corporation
Burlington, Massachusetts 01803
Contract F29601-69-C-0001



TECHNICAL REPORT NO. AFWL-TR-69-87

December 1969

AIR FORCE WEAPONS LABORATORY
Air Force Systems Command
Kirtland Air Force Base
New Mexico

This document has been approved for public release
and sale; its distribution is unlimited.

AIR FORCE WEAPONS LABORATORY
Air Force Systems Command
Kirtland Air Force Base
New Mexico

When U. S. Government drawings, specifications, or other data are used for any purpose other than a definitely related Government procurement operation, the Government thereby incurs no responsibility nor any obligation whatsoever, and the fact that the Government may have formulated, furnished, or in any way supplied the said drawings, specifications, or other data, is not to be regarded by implication or otherwise, as in any manner licensing the holder or any other person or corporation, or conveying any rights or permission to manufacture, use, or sell any patented invention that may in any way be related thereto.

This report is made available for study with the understanding that proprietary interests in and relating thereto will not be impaired. In case of apparent conflict or any other questions between the Government's rights and those of others, notify the Judge Advocate, Air Force Systems Command, Andrews Air Force Base, Washington, D. C. 20331.

DO NOT RETURN THIS COPY. RETAIN OR DESTROY.

LASER-TRIGGERED SWITCHING STUDY

John J. Moriarty

Ion Physics Corporation
Burlington, Massachusetts 01803
Contract F29601-69-C-0001

TECHNICAL REPORT NO. AFWL-TR-69-87

This document has been approved
for public release and sale;
its distribution is unlimited.

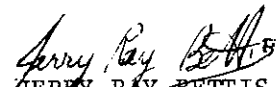
FOREWORD


This report was prepared by Ion Physics Corporation, Burlington, Massachusetts, under Contract F29601-69-C-0001. The research was performed under Program Element 61102H, Project 5710, Subtask RRL 1053, and was funded by the Defense Atomic Support Agency (DASA).


Inclusive dates of research were September 1968 through May 1969. The report was submitted 17 October 1969 by the Air Force Weapons Laboratory Project Officer, Captain Jerry Ray Bettis (WLZS).

This study of laser-triggered multimegavolt switching was carried out in the Technology Division of Ion Physics Corporation by Mr. John J. Moriarty under the supervision of Dr. Helmut Milde. Engineering assistance was provided throughout the program by Mr. Carl Litchfield. The mechanical design was performed by Mr. David Overberg. The success of this program is due in great measure to the assistance rendered by Captain Bettis, Dr. R. V. Wick, and Dr. A. H. Guenther of AFWL who gave generously of their time and equipment.

This technical report has been reviewed and is approved.


JERRY RAY BETTIS
Captain, USAF
Project Officer


RUDY L. VAN HEMERT, Major, USAF
Chief, Simulation Branch


ARTHUR H. GUENTHER
Chief, Technology Division

ABSTRACT

(Distribution Limitation Statement No. 1)

Single- and double-channel laser-triggered switches in high-pressure gas have been designed and operated in the voltage range from 1 MV to more than 3 MV. Jitter times of 1 to 3 ns were observed in most cases. Gas pressures of 150 psig and 300 psig were used. The gases were 100 percent nitrogen and a 4:1 mixture (by partial pressures) of $N_2 + SF_6$ enriched with up to 50 percent argon. Significant accomplishments were (1) the simultaneous firing of four stages of a Marx generator by a multiply split laser-beam; (2) up to 40 percent reduction in the risetime observed in the output pulse from a multimegavolt dc generator when switched into a load through two simultaneously laser-triggered channels; and (3) the design and operation of a laser-triggered, dc-charged switch at more than 3 MV with subnanosecond jitter.

This page intentionally left blank.

TABLE OF CONTENTS

| <u>Section</u> | | <u>Page</u> |
|----------------|---|-------------|
| 1 | INTRODUCTION | 1 |
| 2 | PRELIMINARY SWITCHING EXPERIMENTS | 3 |
| | 2.1 Multiply Triggered Marx Generator | 3 |
| | 2.2 Preparation of Multimegavolt Switching Apparatus | 10 |
| | 2.3 Data Acquisition and Analysis Techniques | 17 |
| | 2.4 Initial Operation of Multimegavolt Laser Switch | 20 |
| 3 | SWITCHING EXPERIMENTS | 23 |
| | 3.1 Single-Channel Switching | 23 |
| | 3.1.1 Delay and Jitter | 23 |
| | 3.1.2 Discharge Characteristics | 33 |
| | 3.2 Double-Channel Switching | 33 |
| | 3.2.1 Observations and Data | 33 |
| | 3.2.2 Characteristic Times for Double- Channel Switching | 37 |
| | 3.2.3 Risetime Considerations | 42 |
| 4 | COMPLEMENTARY RESULTS FROM SIEGE II PROGRAM | 45 |
| 5 | CONCLUSIONS | 55 |
| 6 | REFERENCES | 57 |

APPENDIX

| | |
|---|----|
| CALCULATION OF POWER DENSITY AT TARGET ELECTRODE | 59 |
| DISTRIBUTION | 64 |

LIST OF ILLUSTRATIONS

| <u>Figure</u> | | <u>Page</u> |
|---------------|---|-------------|
| 1 | Giant Pulse Ruby Laser System | 4 |
| 2 | Beam Splitting Apparatus for Triggering Four Gaps Simultaneously | 5 |
| 3 | Schematic of Multiply Split Laser Beam | 6 |
| 4 | Output Pulses from Laser-Triggered Marx Generator | 8 |
| 5 | Laser-Switching System Assembly Drawing | 11 |
| 6 | Baseplate Assembly with Mounted Focusing Lenses | 13 |
| 7 | Beam Splitting Optics Mounted on FX-25 | 15 |
| 8 | Laser-Switch Load Assembly on FX-25 Multi- megavolt Generator | 16 |
| 9 | Laser-Triggered Discharge in Nitrogen | 18 |
| 10 | Oscilloscope Traces for Four Consecutive Laser- Triggered Discharges in Nitrogen | 19 |
| 11 | Switch Delay in N_2 at 50% SBV | 24 |
| 12 | Switch Delay in N_2 at 95% SBV | 25 |
| 13 | Switch Delay in $A + N_2 + SF_6$ at 67% SBV | 27 |
| 14 | Switch Delay in $A + N_2 + SF_6$ at 94% SBV | 28 |
| 15 | Delay Versus Percent Argon at 150 psig | 34 |
| 16 | Jitter Versus Percent Argon at 150 psig | 35 |
| 17 | Laser-Switched Discharges at 300 psig (Single Channel) | 36 |
| 18 | Laser-Switched Discharges at 150 psig (Double Channel) | 38 |
| 19 | Laser-Switched Discharges at 300 psig (Double Channel) | 39 |
| 20 | Diagram of Laser Triggering at 20 m | 46 |
| 21 | Laser-Switch Load Assembly and Turning Prisms | 47 |
| 22 | Apparatus for Laser-Triggering 2-MV Switch Over 20 m Path | 48 |
| 23 | Switch Delay in N_2 at 22 m (100 MW Laser) | 49 |

LIST OF ILLUSTRATIONS (Continued)

| <u>Figure</u> | | <u>Page</u> |
|---------------|--|-------------|
| 24 | Switch Delay in N_2 at 22 m (125 MW Laser) | 50 |
| A-1 | Gaussian Beam Transformed by a Lens | A-2 |
| A-2 | Beam Divergence of K-1500 Laser System | A-4 |

LIST OF TABLES

| <u>Table</u> | | <u>Page</u> |
|--------------|--|-------------|
| 1 | Delay and Risetime in a Laser-Triggered Marx Generator | 9 |
| 2 | Switching Results in 100% Nitrogen | 29 |
| 3 | Switching Results in Various Gas Mixtures | 30 |
| 4 | Effect of Laser Power Density on Delay and Jitter | 31 |
| 5 | Effect of Gap Separation on Delay and Jitter | 32 |
| 6 | Double-Channel Switching Results | 40 |
| 7 | Calculated Risetimes and Time Constants | 43 |
| 8 | Effect of Laser-to-Switch Separation | 52 |
| A-1 | Power Densities at Target | A-5 |

SECTION I INTRODUCTION

The primary objective of this study has been to extend the laser-triggered switching technology developed by the Air Force Weapons Laboratory into the multimegavolt region. This objective has been satisfied; the validity of the predictions of low jitter switching based on the earlier work of Guenther and his colleagues^(1, 2, 3) at AFWL has been demonstrated at voltages in excess of 3 MV.

A compelling reason for investigating this form of switching is its potential application in the development of devices for the simulation of nuclear detonations. Such devices may require that several energy stores be switched simultaneously into a load requiring power in excess of that available from a single store of compatible impedance.

The magnitude of the parameters necessary to satisfy this application would make the following demands on the switch:

- (1) Voltage hold-off > 10 MV
- (2) Current > 1 MA
- (3) Jitter < 2 ns
- (4) Very low inductance leading to a risetime of a few ns.

A high-pressure gas-filled switch operated under dc conditions and triggered by means of a focused optical beam from a high-brightness laser has been developed at AFWL. The experiments of Guenther and Bettis⁽³⁾ with this switch at voltages extending to 1.2 MV indicate that it will be able to meet the demands above.

A significant step toward these goals has been accomplished by IPC in the present study in which experiments were performed on a high pressure gas-filled spark gap fed by an energy store capable of supplying current and voltage in excess of 50 kA at more than 3 MV. The generating system used was an IPC facility designated FX-25. The reduction of inductance and, consequently,

risetime, by means of double-channel initiation was investigated. The effects of gas composition and pressure, electrode spacing, reduced electric field (E/p) and charging polarity were examined.

The effects of laser power density at the target and the cone angle of the focused beam were studied. This portion of the investigation was augmented by extending the time of performance of this study to coincide with a related program⁽⁴⁾ in which a 2-MV gap was triggered by a laser beam which had traversed a 20-m path.

A demonstration of the effect of the simultaneous switching of several gaps by means of a multiply split laser beam was performed on a Marx Surge Generator. The output risetime and delay were measured as a function of the number of gaps irradiated and the gap voltage.

The experimental work is described in the following three sections of this report. The first, Section 2, describes preliminary efforts with the Marx generator and the initial multimegavolt setup on the FX-25 facility. The apparatus, data taking and data analysis procedures are also described in this section. In Section 3 the principal switching experiments are reported. Most of the results are based on this series of experiments. Pertinent results from the complementary study performed during the SIEGE II⁽⁴⁾ program are summarized in Section 4.

A calculation of power density at the target is described in the Appendix. This calculation takes into account both the vertical and horizontal beam divergence of the laser, and follows Kogelnik's⁽⁵⁾ analysis of the passage of Gaussian beams through lenses.

SECTION 2

PRELIMINARY SWITCHING EXPERIMENTS

This section describes some of the experimental work performed in preparation for the multimegavolt experiments as well as a demonstration of the potential application of the simultaneous laser-triggering of several spark gaps.

A substantial effort was expended in the design, fabrication and testing of the beam-handling apparatus and modified spark gap required for multimegavolt experiments on the Company's FX-25 facility. In the meantime the IPC staff assigned to this program, with the aid of AFWL personnel, set up and gained familiarity with the Korad K-1500 laser system provided by AFWL and shown in Figure 1.

This system employs ruby oscillator and amplifier rods and is Q-switched by means of a Pockels cell. The output face of the amplifier is cut at the Brewster angle to minimize reflections, and produces an elliptically shaped beam approximately 2 cm by 1 cm. During these experiments an output power of 100 MW to 300 MW was obtained in pulses ~ 15 ns wide (FWHM) at 6943 Å. Input energy to the flashlamps was between 10 and 15 kJ.

2.1 Multiply Triggered Marx Generator

The first laser switching experiments at IPC were performed on a five-stage Marx generator, each stage consisting of a 4000 pF capacitor charged to approximately 25 kV. As many as four stages could be triggered by means of a single laser pulse split into four focused beams on passing through the array of beam splitters, prisms and lenses shown in Figure 2. The beams were incident obliquely on the grounded electrode of each gap as shown schematically in Figure 3.

Observations were made for charging voltages of 70% to 90% of the gap static breakdown voltage (SBV). Laser power was varied from 10 MW to 20 MW per gap in 30 ns wide (FWHM) pulses. A small fraction of the incident laser pulse was sampled by an ITT FW-114A biplanar photodiode.

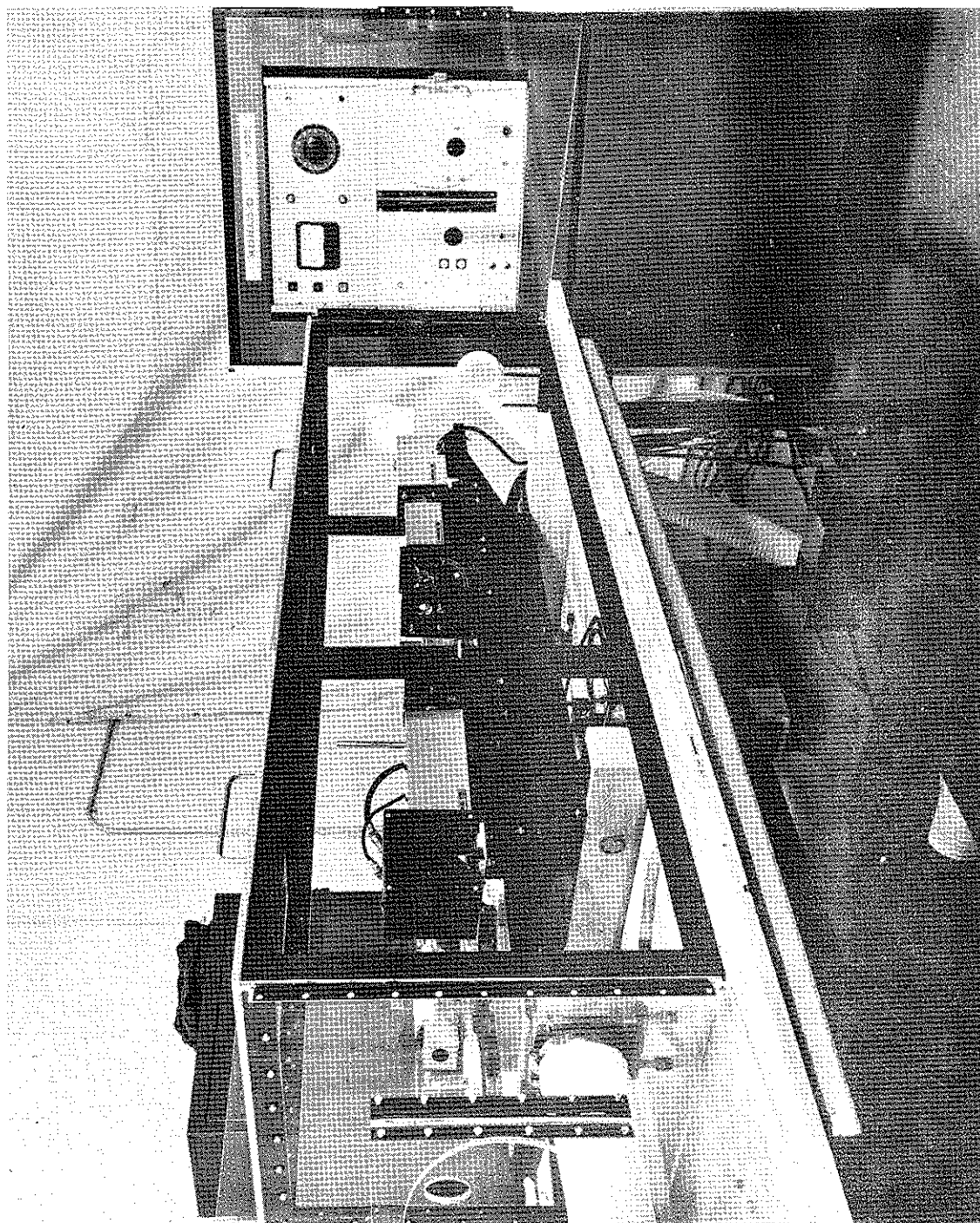


Figure 1. Giant Pulse Ruby Laser System



Figure 2. Beam Splitting Apparatus for Triggering
Four Gaps Simultaneously

2-1126

1-3369a

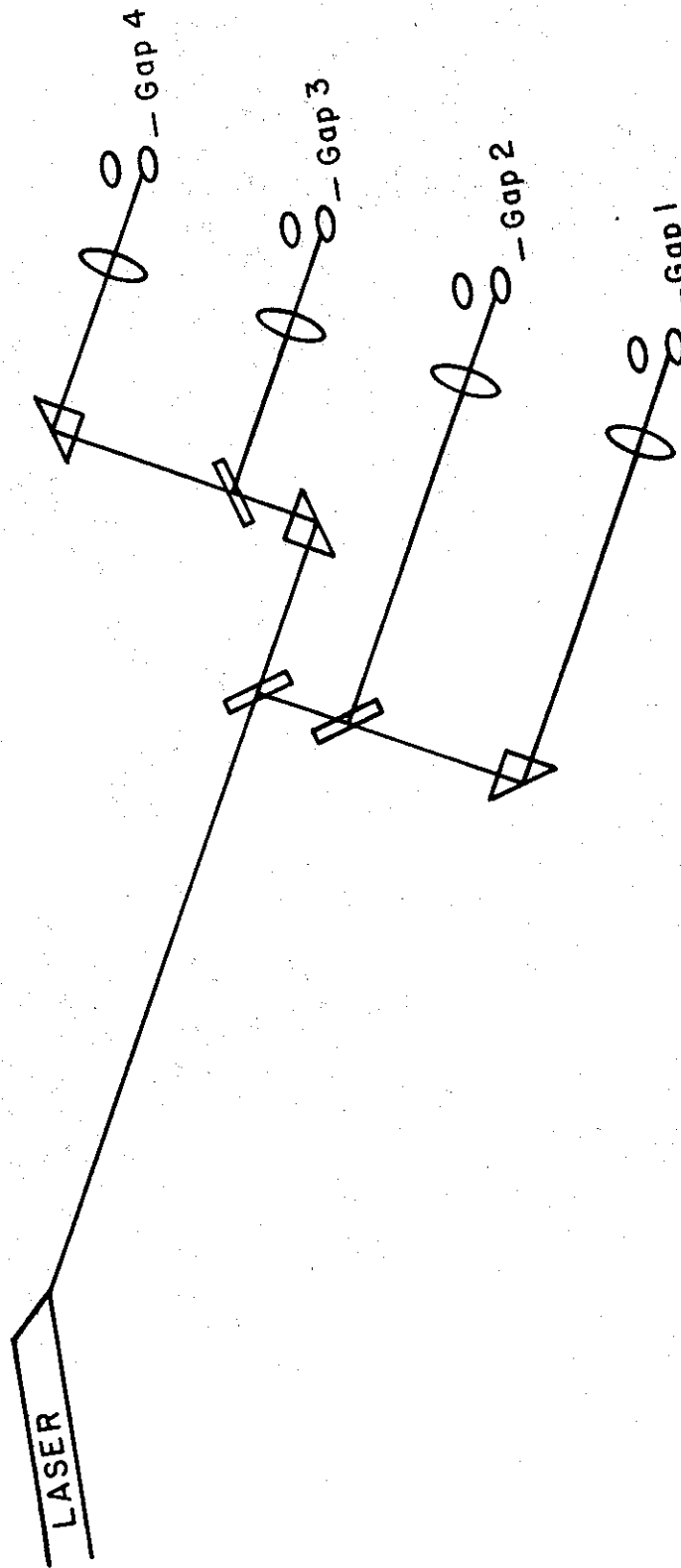


Figure 3. Schematic of Multiply Split Laser Beam

Another small fraction of the laser output was sampled by a foil calorimeter⁽⁶⁾ whose output voltage was monitored on a Keithly Model 150A Microvolt Ammeter adapted for use with a Westronics Model D5A/M/D141 M Recorder. This energy sensing device was calibrated against a TRG Model 117 Ballistic Thermopile. From the pulsewidth and energy thus obtained, the peak laser output power was calculated. The output of the Marx was monitored by means of a resistive voltage divider. The two pulses were combined in a matched signal splitter* and displayed on a Tektronix 519 oscilloscope. Delay between the incidence of the laser pulses at the gaps and the output of the Marx was determined by correcting for cable lengths and time-of-flight of the light beams as in Reference 3. The transit times from the laser to all four gaps were equal within 0.5 ns.

A sample of these data in Figure 4 reveals the effect of the number of triggered gaps on both delay and risetime of the Marx output. Each stage was charged to -27 kV which was 90% of SBV. Only 10 MW laser power per gap was required. As the operating voltage was reduced to lower percentages of static breakdown an increase in laser power was required to keep the delay within measurable bounds. At 70% SBV only one observation of the Marx output was found. It was verified that the Marx did fire by means of a voltmeter across one of the stages. It is likely that the delay was too long to allow measurement with the apparatus employed. Further increase in laser power to decrease delay was not possible at this time.

The results summarized in Table 1 indicate the decrease in delay and increase in risetime with an increasing number of triggered gaps. Although the triggering delay of the Marx can be reduced by firing all the gaps simultaneously, a slower risetime is observed. It would be interesting to investigate this behavior in more detail to determine whether the multiple overvolting of the upper stages of the conventional Marx or the early establishment of a suitable current in the individual Marx stages is the decisive factor which controls the risetime of the output pulse.

* Bishop Instrument Model 080-001, Portland Maine

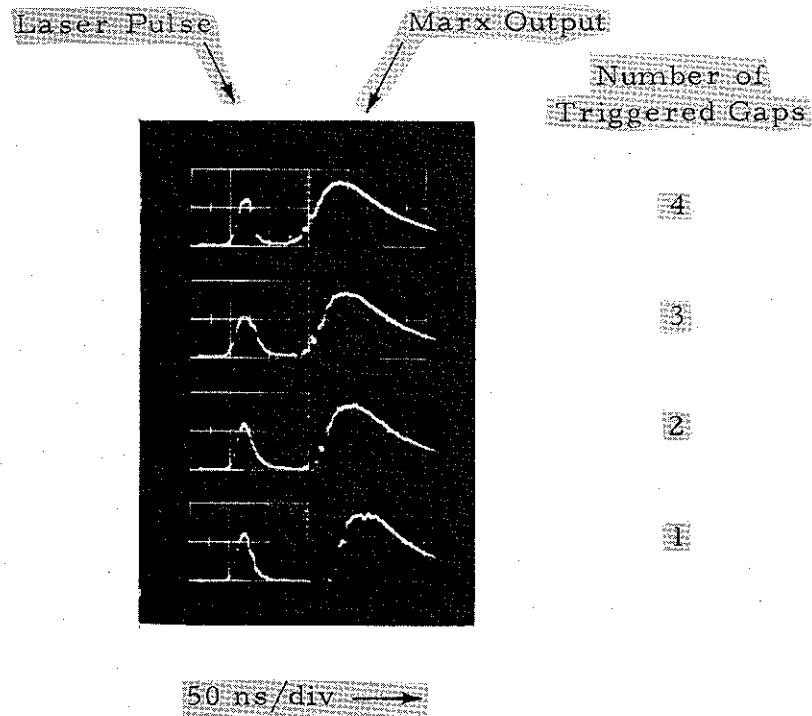


Figure 4. Output Pulses from Laser-Triggered Marx Generator

2-1121

Table 1. Delay and Risettime in a Laser-Triggered Marx Generator

| Gap Voltage | % SBV | Laser Power/Gap | Number of Triggered Gaps | Delay (ns) | 10-90% Risettime (ns) |
|-------------|-------|-----------------|--------------------------|------------|-----------------------|
| -26.5 kV | 90% | 10 MW | 1 | 124 | 18 |
| | | | 2 | 74 | 22 |
| | | | 3 | 59 | 29 |
| | | | 4 | 49 | 31 |
| -24 kV | 80% | 20 MW | 1 | 90 | 9 |
| | | | 2 | 53 | 11 |
| | | | 3 | 45 | 12 |
| | | | 4 | 36 | 14 |
| -21 kV | 70% | 20 MW | 4 | 219 | 30 |

Because of the difference in laser power levels it is not possible to compare the absolute values of delay and risetime observed at the different percentages of SBV.

Investigation of the Marx triggering was interrupted at this point because of the failure of the Pockels shutter electronics. This failure and an aged oscillator flashlamp were responsible for the wide pulses (30 ns) and low powers obtained from the laser during the experiments. By the time the laser system was repaired the apparatus for multimegavolt switching on FX-25 was ready for installation and testing. Therefore, the Marx triggering experiments were terminated.

2.2 Preparation of Multimegavolt Switching Apparatus

The IPC FX-25 facility provides energy storage of about 5 kJ at voltages in excess of 3 MV. The system consists of a pressurized coaxial capacitor dc charged by a Van de Graaff generator. The energy is transferred to a load by switching the center conductor terminal across a gap to an electrode isolated from ground by a 60 to 90 ohm copper sulfate load.

A sketch of some of the apparatus we have used to study the laser switching technique is shown in Figure 5. This drawing shows the assembly of the laser beam entrance channel, resistive load, window and focusing lens at the high-voltage terminal end of the FX-25 flash X-ray machine. Complete assembly drawings and parts lists were included in an earlier report.⁽⁷⁾

The laser beam enters at the right hand side of the drawing, passes through a pressure-tight window in the baseplate and is focused on a target inserted in the terminal electrode. The baseplate assembly is shown partly assembled in Figure 6. Three focusing lenses are mounted on this plate in adjustable barrels such that the beam or beams can be brought to a focus at positions ranging from 2 cm in front of the targets to 1.5 mm inside the

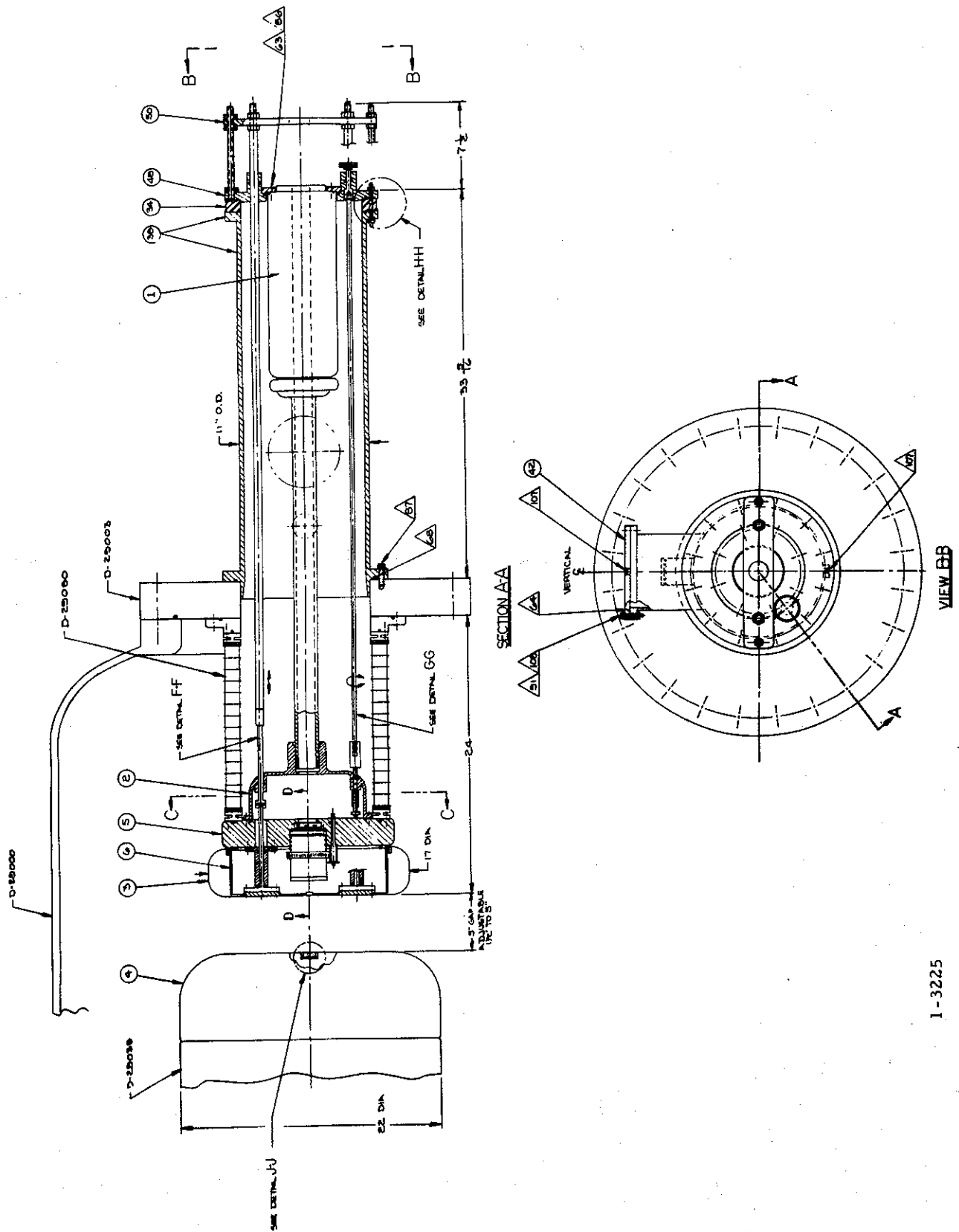


Figure 5. Laser-Switching System Assembly Drawing

1-3225

This page intentionally left blank.

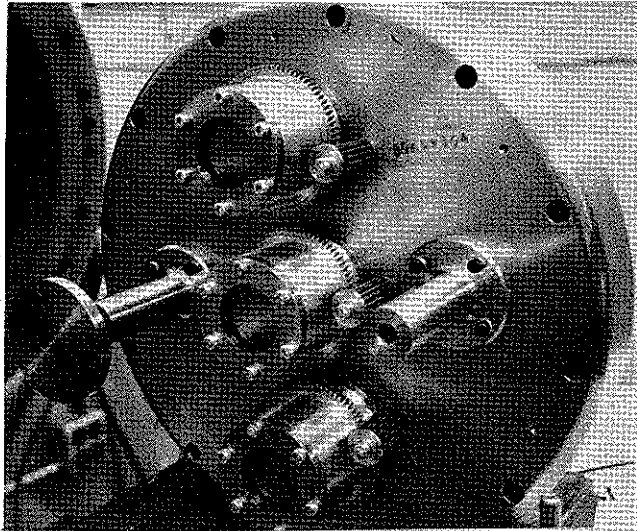


Figure 6. Baseplate Assembly with Mounted Focusing Lenses

2-1313

target(s). The targets are made from a sintered copper-tungsten composite manufactured under the tradename* Elkonite.

Three focusing lenses were installed so that the apparatus could be operated in either the single-channel or the double-channel mode without disassembly. The beam-splitting optics are shown in Figure 7 mounted on the baseplate (opposite side from that shown in Figure 6) which has been attached to the insulating housing (rings) of the FX-25. The geared drive on the beam-splitter carriage can be operated from outside the entire sealed assembly to move the beam splitter to the left for single-channel operation or to the center, as shown, for the double-channel mode. Three 90-degree turning prisms complete the beam handling apparatus. All optical components are made from GE151 fused silica, and all appropriate surfaces are anti-reflection coated for $< 0.15\%$ reflectivity at 6943 \AA . An exception was a thin, uncoated dust cover of Corning 7910 glass (UV grade) which was inserted in the beam input channel during some of the experiments. The transmission of the entire assembly was checked with a TRG 117 ballistic thermopile and losses in the dust covers have been accounted for in reporting the laser power into the gap.

The complete assembly of laser-switching load chamber on the FX-25 facility is shown in Figure 8. It had been planned that the load chamber would be insulated with oil, resulting in a load impedance of 60 ohms. However, during the initial testing of our apparatus considerable difficulty was experienced in eliminating all traces of air bubbles from the oil. Therefore, in the interest of expediting the experimental work, the load chamber was insulated by pressurization to three atmospheres of SF_6 , resulting in a load impedance of 90 ohms. The copper sulfate load resistor was modified to match this impedance.

* Mallory Metallurgical Company, Indianapolis, Indiana

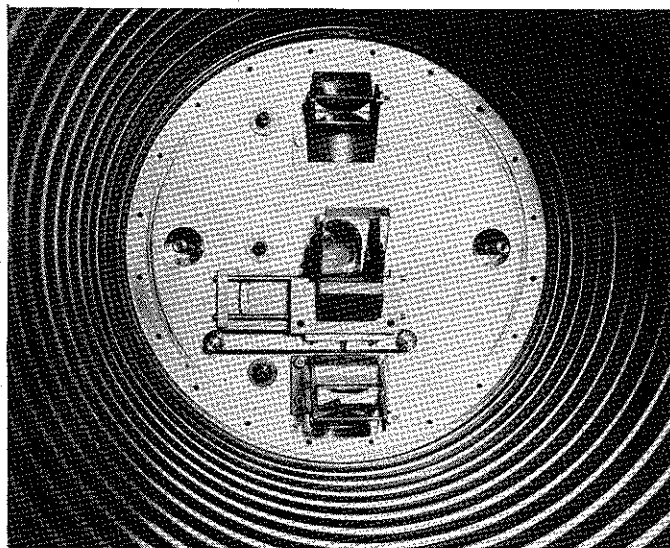


Figure 7. Beam Splitting Optics
Mounted on FX-25

2-1314

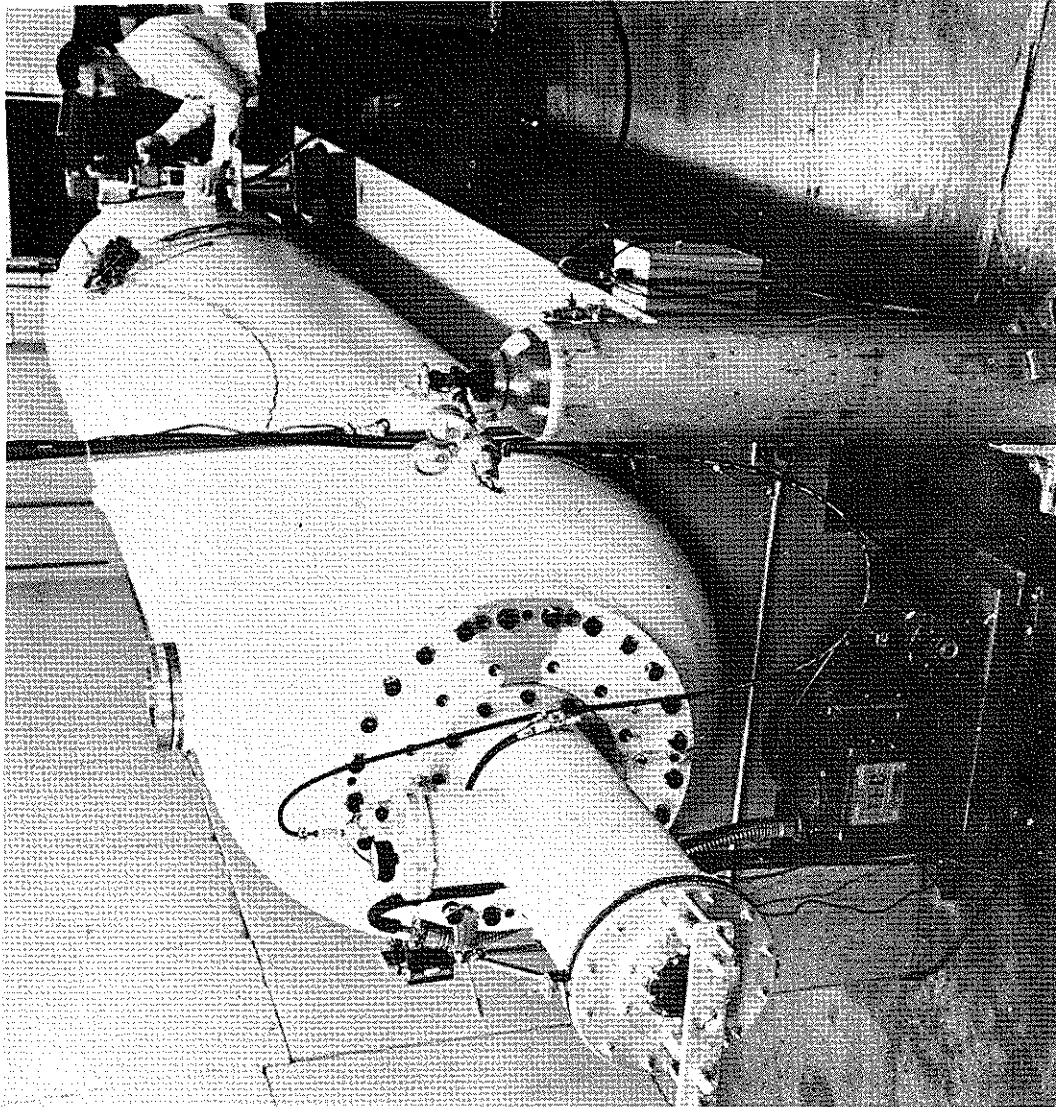


Figure 8. Laser-Switch Load Assembly
on FX-25 Multimegavolt Generator

The aim of these experiments was the characterization of multi-megavolt laser switch operation in terms of gap and laser parameters. It was necessary, therefore, to specify the following:

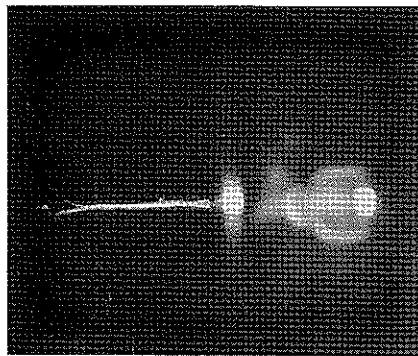
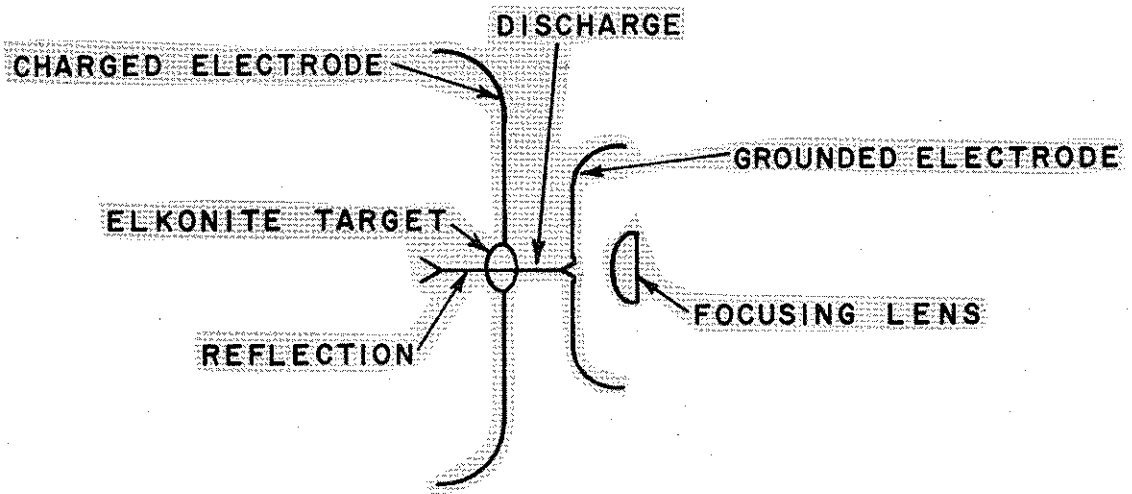
- (1) Gap parameters:
 - (a) gas composition and pressure
 - (b) electrode separation and material
 - (c) static breakdown voltage
 - (d) operating voltage
- (2) Laser parameters:
 - (a) output energy and wavelength
 - (b) pulse width (FWHM)
 - (c) beam divergence and focusing optics

From this information was calculated:

- (1) reduced electric field (E/p)
- (2) % SBV at switch firing
- (3) laser power density at target surface

The data taken for each shot included a still photograph of the breakdown and a photograph of an oscilloscope trace containing both the laser pulse and a voltage pulse. An example of these data is shown in Figures 9 and 10. The bright glare in Figure 9 is due to a reflection from the electrode during pre-exposure of the background with a strobe flash.

The pulses shown in Figure 10 were obtained from the photodiode described earlier and a capacitive voltage probe in the terminating load housing. Both signals were combined in the matched signal splitter and displayed on a Tektronix 519 oscilloscope. Wherever possible, the 10 ns/cm scale was used. Tangent lines were drawn along the leading edge of each pulse and the delay was measured between their intersections at the baseline. These values were



Shot No. 121

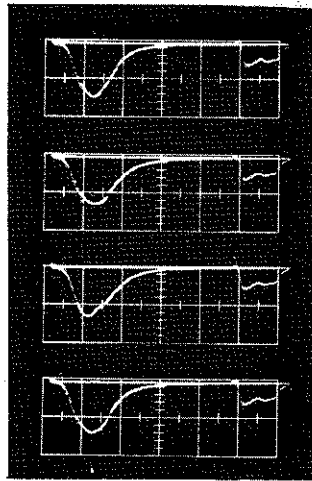
Figure 9. Laser-Triggered Discharge in Nitrogen

2-1275

Inverted Laser Pulse

Negative Voltage Pulse

Shot No.



121

122

123

124

20 ns/div

Figure 10. Oscilloscope Traces for Four Consecutive Laser-Triggered Discharges in Nitrogen

2-1276

corrected for differences in cable lengths and time of flight of the laser beam from the photodiode to the target. The absolute values of delay measured in this way are assumed to be accurate to 1 ns for data read from the 10 ns/cm scale.

Usually 10 to 20 shots were taken for each set of operating parameters. The resulting delay data were analyzed by means of a computer program which calculated the arithmetic mean delay and standard deviation, defined as the "rms jitter." Unbiased estimates of population parameters were used in the calculation, which resulted in slightly larger jitter values than estimating standard deviation by "maximum likelihood."⁽⁸⁾

2.4 Initial Operation of Multimegavolt Laser Switch

During initial operation of this apparatus adjustments were necessary in the focusing and beam alignment techniques and minimization of the beam divergence of the laser system. Nevertheless, even before the system was optimized a gap was fired several times at nearly 3 MV by means of the focused laser beam. Optimization of the system was accomplished by minimizing the beam divergence by means of precise positioning of the beam expanding optics between laser oscillator and amplifier. The divergence was then measured by Winer's⁽⁹⁾ photographic technique. These data, processed and analyzed at AFWL, are presented in the Appendix together with a calculation of the spot size and resultant power density at the electrode. For the operating range utilized in our experiments the full angle beam divergence was generally less than 1.5 mrad.

Initial megavolt switching was performed in 100% nitrogen at 350 psig with the geometric focal spot of the lens set 1 cm in front of the target. Very high powers were required to switch the gap under these conditions. Switching delay observed in a 6-cm gap operated at 2 MV (>95% SBV) was 15.3 ± 1.4 ns with 300 MW of laser power. Since it had already been observed in the prior work at AFWL that more reliable results could be obtained with

the laser beam focused just beneath the surface of the target no further data were taken with this focal adjustment. All subsequent measurements were made with the geometric focal spot of the lens set 1.5 mm inside the target. This proved to be a more efficient triggering arrangement, as is evident from the shorter delays observed with lower laser powers under fairly similar gap conditions described in the following sections.

This page intentionally left blank.

SECTION 3

SWITCHING EXPERIMENTS

These experiments resulted in delay and jitter values for switching with various gas mixtures, pressures, gap separations and terminal voltages. The approach taken was an exploratory one in which several gas mixtures were studied briefly rather than a more detailed examination of only one or two combinations.

A number of data points (usually 10 to 20) were averaged for each reported value of delay. Although double-channel switching was observed over the entire voltage range, the bulk of the effort was expended on single-channel observations.

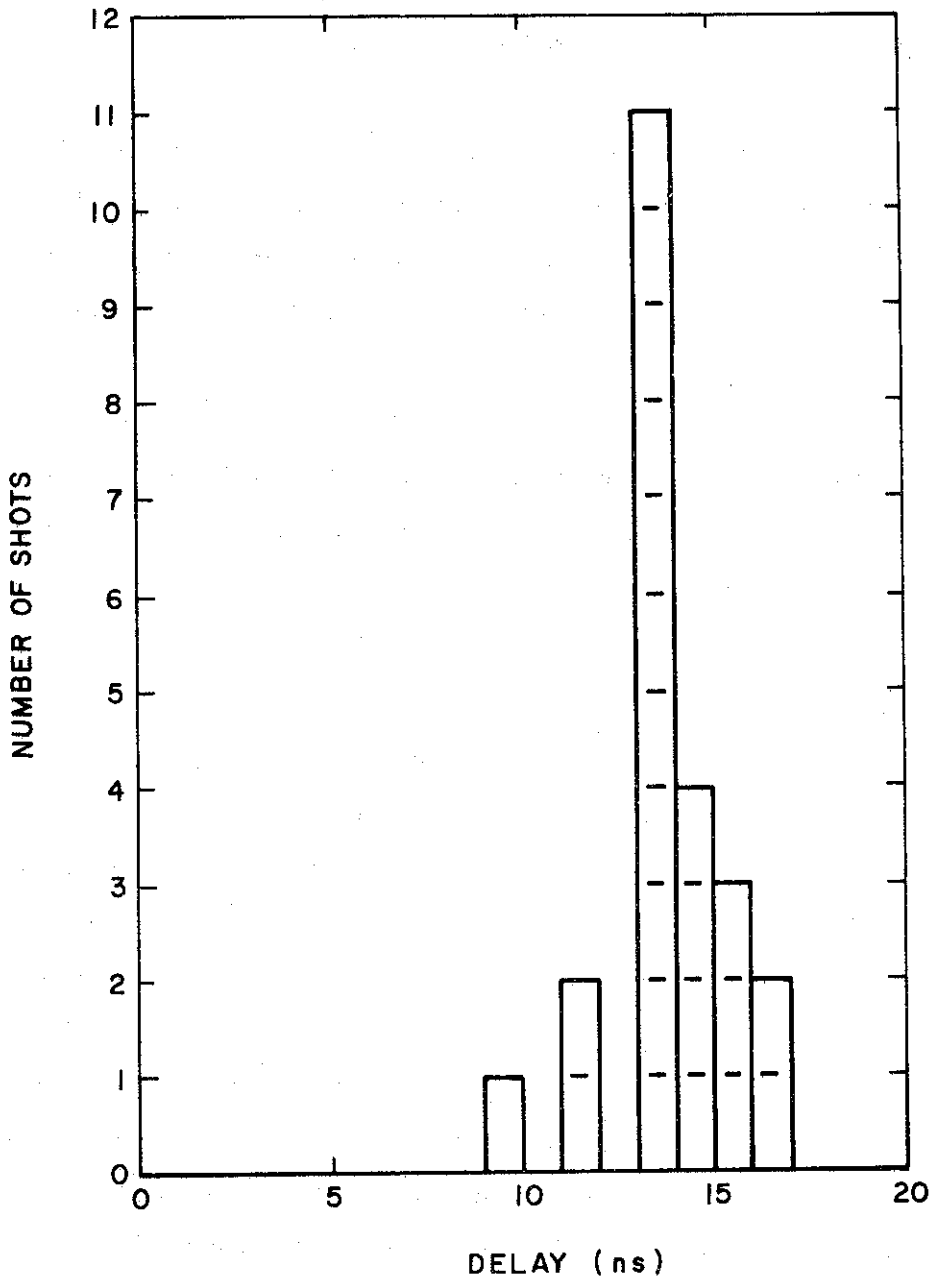
3.1 Single-Channel Switching

These experiments were carried out at two operating levels of the laser system, namely 100 MW and 200 MW. Because of transmission losses in two uncoated dust shields, the actual power transmitted to the gap in these cases was 85 and 160 MW, respectively. The accuracy of the power quoted is limited by the fluctuations in laser output and the accuracy of the recording devices to about $\pm 10\%$.

Since beam divergence varies with the operating level of the laser system, the power density at the electrode provides a more exact characterization of switch operation than the incident power. The two power levels used in this series of experiments resulted in power densities of 65 GW/cm^2 and 164 GW/cm^2 . The greater than expected increase in power density at the higher operating level was due in part to a decrease in beam divergence at this level, as shown in Figure A-2 of the Appendix.

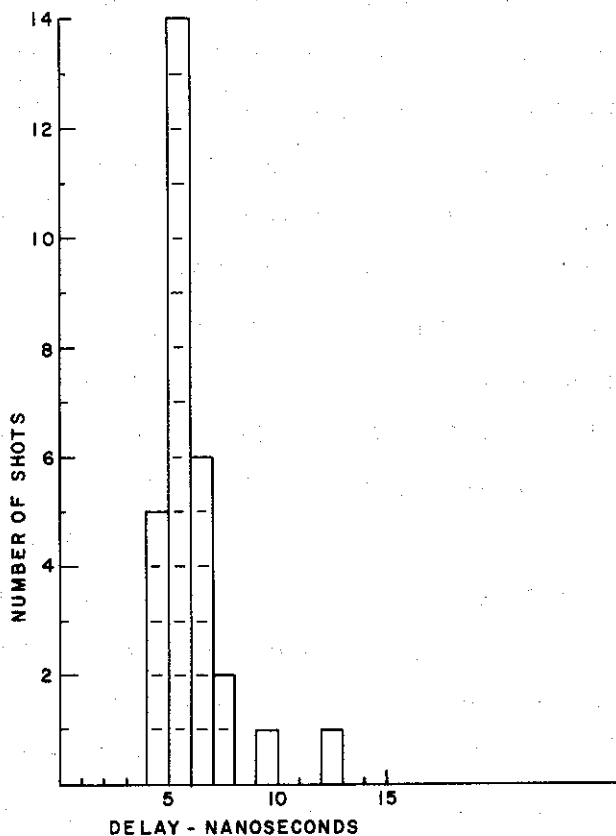
3.1.1 Delay and Jitter

Some of the delay measurements in nitrogen are presented as histograms in Figures 11 and 12. The mean delays and standard deviations.



Gas: 150 psig, 100% N₂, Gap: 7 cm
 Terminal: + 1.05 MV, 50% SBV
 E/P = 17.6 V/cm torr
 Laser Power: 85 MW

Figure 11. Switch Delay in N₂ at 50% SBV



Gas: 150 psig, 100% N₂, Gap: 7cm
 Terminal: + 1.9 MV, 95% SBV
 E/p = 31.9 V/cm torr
 Laser Power: 160 MW

Figure 12. Switch Delay in N₂ at 95% SBV

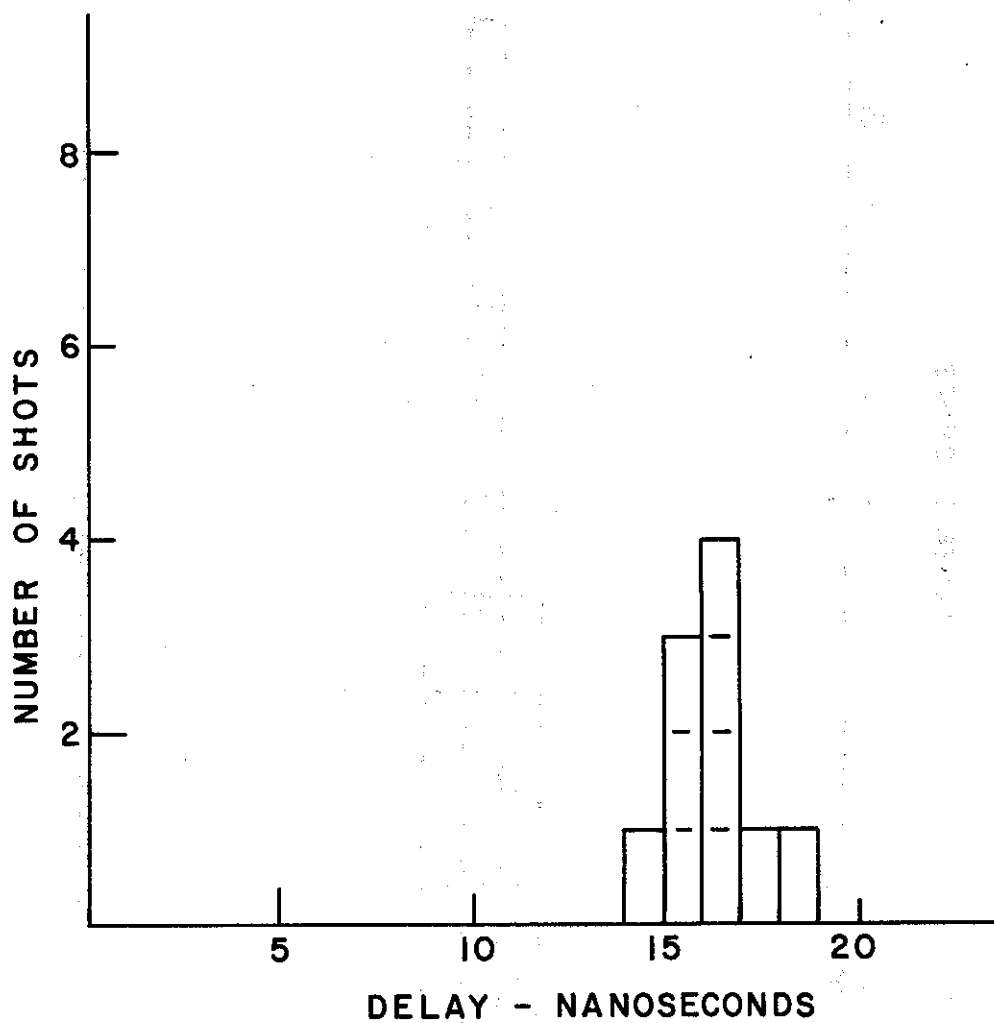
(rms jitter) calculated from these data are 14.3 ± 1.6 ns for the 50% SBV case and 6.6 ± 1.6 ns for 95% SBV. The power densities used were 65 GW/cm^2 in the former and 164 GW/cm^2 in the latter.

The addition of 20% SF_6 (by partial pressure) resulted in very poor switching operation. Data obtained at the lower power were too scattered to analyze. In an effort to find a gas mixture with good switching characteristics as well as good voltage holdoff capability, increasing percentages of argon were added to the basic 4:1 mixture of nitrogen and SF_6 . Substantial improvement in switching was obtained in a 3.25 MV gap with mixture of 50% A, 40% N_2 and 10% SF_6 . Histograms of these data are given in Figures 13 and 14. The delays and jitters calculated from these data are 16.8 ± 1.1 ns for 67% SBV and 10.0 ± 0.7 ns at 94% SBV. These standard deviations are very close to the limit of accuracy for delay measurement stated earlier.

The results of the entire series of measurements in nitrogen are presented in Table 1; those for the gas mixtures are in Table 3. For two of the cases listed in Table 2 some misfires are noted. These shots were not counted as measurements in the tabulations. In the cases where all but one parameter remains essentially constant, these results can be grouped so as to show the effect of gap separation, laser power density and gas composition on delay and jitter.

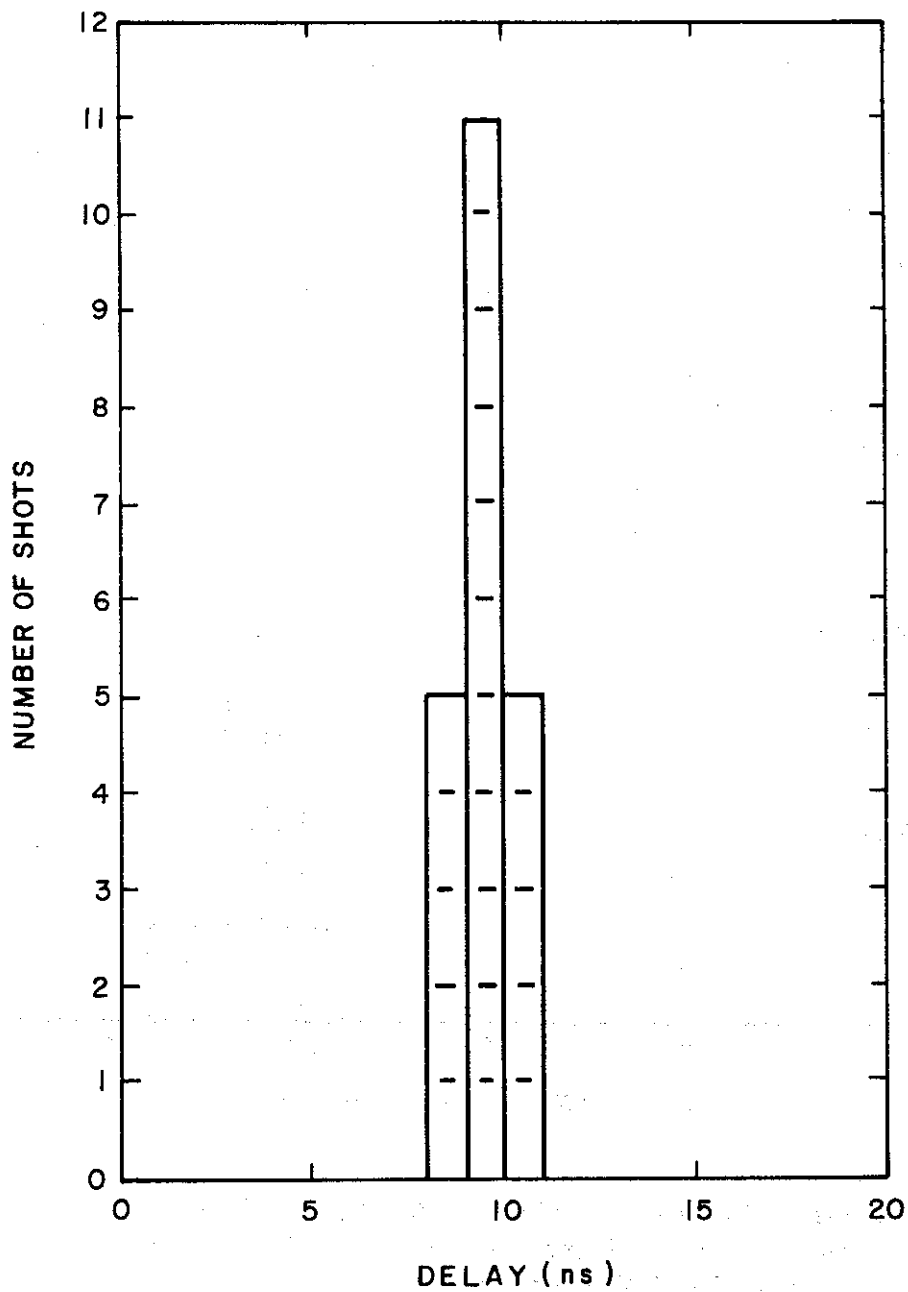
The effect of laser power density is shown for nitrogen and two gas mixtures in Table 4. When delay is comparable to or greater than the laser pulse width (~ 15 ns FWHM) an improvement is obtained at the higher laser power. However, when switching is complete before the laser pulse has reached its maximum level, increased laser power brings no improvement. This is clearly evident in the comparative delay data for a 7-cm gap in nitrogen at 150 psig. Switching is complete in this gap before the lower power pulse has reached half its maximum value. The values of delay and jitter observed for the two power levels agree within the experimental limit of error.

The effect of gap separation on delay and jitter of a multimegavolt switch is given in Table 5. As expected, delay increases with gap separation when other parameters are held constant.



Gas: 300 psig, 50% A + 40% N₂ + 10% SF₆
 Gap: 11 cm, Terminal: + 2.1 MV, 67% SBV
 E/p = 11.7 V/cm torr
 Laser Power: 160 MW

Figure 13. Switch Delay in A + N₂ + SF₆ at 67% SBV



Gas: 300 psig, 50% A, 40% N₂, 10% SF₆
 Gap: 11 cm; Terminal: + 3.05 MV, 94% SBV
 E/P = 17.4 V/cm torr; Laser Power: 160 MW

Figure 14. Switch Delay in A+N₂+SF₆ at 94% SBV

1-3537

Table 2. Switching Results in 100% Nitrogen

| Pressure psig | Voltage MV | Gap cm | % of SBV | E/P V/cm torr | Number of measure- ments | Delay ns | Jitter ns | Laser Power Density GW/cm ² |
|------------------|---------------|-----------|----------------|---------------------|-----------------------------------|-------------|--------------|---|
| 300 | +2.1 | 7 | 91 | 18.4 | 12 | 7.8 | ±3.4 | 164 |
| 300 | +3.15 | 11 | 94 | 17.6 | 10 | 10.0 | ±3.5 | 164 |
| 150 | +2.73 | 11 | 93 | 29.1 | 5 | 11.6 | ±2.2 | 164 |
| 150 | +1.05 | 4 | 83 | 30.9 | 3 | 6.0 | - | 164 |
| 150 | +1.9 | 7 | 95 | 31.9 | 30 | 6.6 | ±1.6 | 164 |
| 300 | +2.1 | 7 | 91 | 18.4 | 9 | 14.7 | ±5.8 | 65 |
| 150 | +2.73 | 11 | 92 | 29.1 | 12 | 14.7 | ±3.2 | 65 |
| 150 | +1.05 | 7 | 50 | 17.6 | 23 | 14.3 | ±1.6 | 65 |
| 150 | +1.9 | 7 | 95 | 31.9 | 18 | 5.3 | ±1.4 | 65 |
| 150 | -1.9 | 7 | 95 | 31.9 | 16 | 6.2 | ±1.4 | 65 |

Table 3. Switching Results in Various Gas Mixtures

| Gas Composition % Argon in $4 N_2 + 1 SF_6$ | Pressure psig | Voltage MV | Gap cm | % of SBV | E/P V/cm torr | Number of Measure- ments | Delay ns | Jitter ns | Laser Power Density GW/cm ² |
|---|------------------|---------------|-----------|----------|---------------------|--------------------------------|-------------|--------------|---|
| 0 | 150 | +2.1 | 7 | 93 | 35.2 | 17 | 12.7 | ±2.7 | 164 |
| 20 | 150 | +1.9 | 7 | 90 | 31.9 | 20 | 11.5 | ±2.6 | 164 |
| 33 | 150 | +1.9 | 7 | 95 | 31.9 | 16 | 13.9 | ±5.3 | 65 |
| 33 | 150 | +1.05 | 7 | 50 | 17.6 | 9 (3 misfires) | 26.1 | ±9.6 | 65 |
| 33 | 150 | +1.9 | 7 | 95 | 31.9 | 20 | 10.0 | ±2.5 | 164 |
| 33 | 150 | -1.55 | 7 | 86 | 26.0 | 22 | 10.1 | ±2.2 | 164 |
| 33 | 150 | +1.05 | 7 | 50 | 17.6 | 12 | 18.8 | ±1.8 | 164 |
| 50 | 150 | +1.55 | 7 | 83 | 26.0 | 21 | 18.0 | ±7.1 | 65 |
| 50 | 150 | +1.6 | 7 | 84 | 26.8 | 20 | 9.8 | ±1.8 | 164 |
| 50 | 150 | +1.1 | 7 | 58 | 18.5 | 20 (1 misfire) | 18.3 | ±4.3 | 164 |
| 50 | 300 | +1.9 | 7 | 83 | 16.6 | 13 | 10.2 | ±1.7 | 164 |
| 50 | 300 | +3.05 | 11 | 94 | 17.0 | 21 | 10.0 | ±0.7 | 164 |
| 50 | 300 | +2.1 | 11 | 67 | 11.7 | 10 | 16.8 | ±1.1 | 164 |

Table 4. Effect of Laser Power Density
on Delay and Jitter

| Gas | E/p (V/cm-torr) | Pressure (psig) | Gap (cm) | % SBV | Delay (ns) | |
|---|--------------------|--------------------|-------------|-------|-----------------------|------------------------|
| | | | | | 65 GW/cm ² | 164 GW/cm ² |
| 100% N ₂ | 18.4 | 300 | 7 | 91 | 14.7 ± 5.8 | 7.8 ± 3.4 |
| | 29.1 | 150 | 11 | 93 | 14.7 ± 3.2 | 11.6 ± 2.2 |
| | 31.9 | 150 | 7 | 95 | 5.3 ± 1.4 | 6.6 ± 1.6 |
| 33% A+ 53% N ₂ + 13% SF ₆ | 31.9 | 150 | 7 | 95 | 13.9 ± 5.3 | 10.0 ± 2.5 |
| | | | | | | |
| 50% A+ 40% N ₂ + 10% SF ₆ | 26-27 | 150 | 7 | 83-84 | 18.0 ± 7.1 | 9.8 ± 1.8 |

Table 5. Effect of Gap Separation
on Delay and Jitter

| Gas | E/p (V/cm-torr) | Pressure (psig) | % SBV | Laser Power (MW) | Delay (ns) | |
|---------------------|--------------------|--------------------|-------|------------------------|------------|------------|
| | | | | | 7 cm Gap | 11 cm Gap |
| 100% N ₂ | 17.6 - 18.4 | 300 | 91-94 | 160 | 7.8 ± 3.4 | 10.0 ± 3.5 |
| | 29.1 - 31.9 | 150 | 93-95 | 160 | 6.6 ± 1.6 | 11.6 ± 2.2 |
| | 29.1 - 31.9 | 150 | 93-95 | 85 | 5.3 ± 1.4 | 14.7 ± 3.2 |

The variations of delay and jitter with increasing percentages of argon in a 4:1 mixture of nitrogen and SF₆ are shown in Figures 15 and 16. A reduction in delay and jitter is obtained as the argon concentration is enriched. This follows from argon's smaller elastic collision probability,⁽¹⁰⁾ larger cross sections for photo-absorption⁽¹¹⁾ and ionization by electron impact,⁽¹²⁾ and has been reported by Guenther⁽¹³⁾ in repetitive laser switching studies.

3. 1. 2 Discharge Characteristics

Photographs of the gap breakdown show the single-channel breakdown characteristics of co-axial laser switching at the smaller gap separation. However, at larger gap separations the single channel divides part way over into many leaders to bridge the gap. Some filaments are observed in both cases near the grounded electrode completing the circuit around the entrance beam aperture. The size of this aperture was reduced from a diameter of 1-1/4 to 9/16 inch with no essential change in the channel fragmentation at wide gaps.

A few of the discharges are shown in Figure 17. Note the different discharge geometry at the 7-cm and 11-cm gap separation. All of the photographs have been inserted in the laboratory notebooks submitted with this report.

3. 2 Double-Channel Switching

By means of the beam splitter and prisms described earlier it was possible to divide the incident laser beam into two beams of equal power which were separately focused on two additional Elkonite targets. These targets were spaced symmetrically above and below the central target on a 25-cm diameter circle on the high voltage terminal.

3. 2. 1 Observations and Data

Double channel switching was observed in nitrogen as well as in a gas mixture of 50% A + 40% N₂ + 10% SF₆. Photographs of some of these

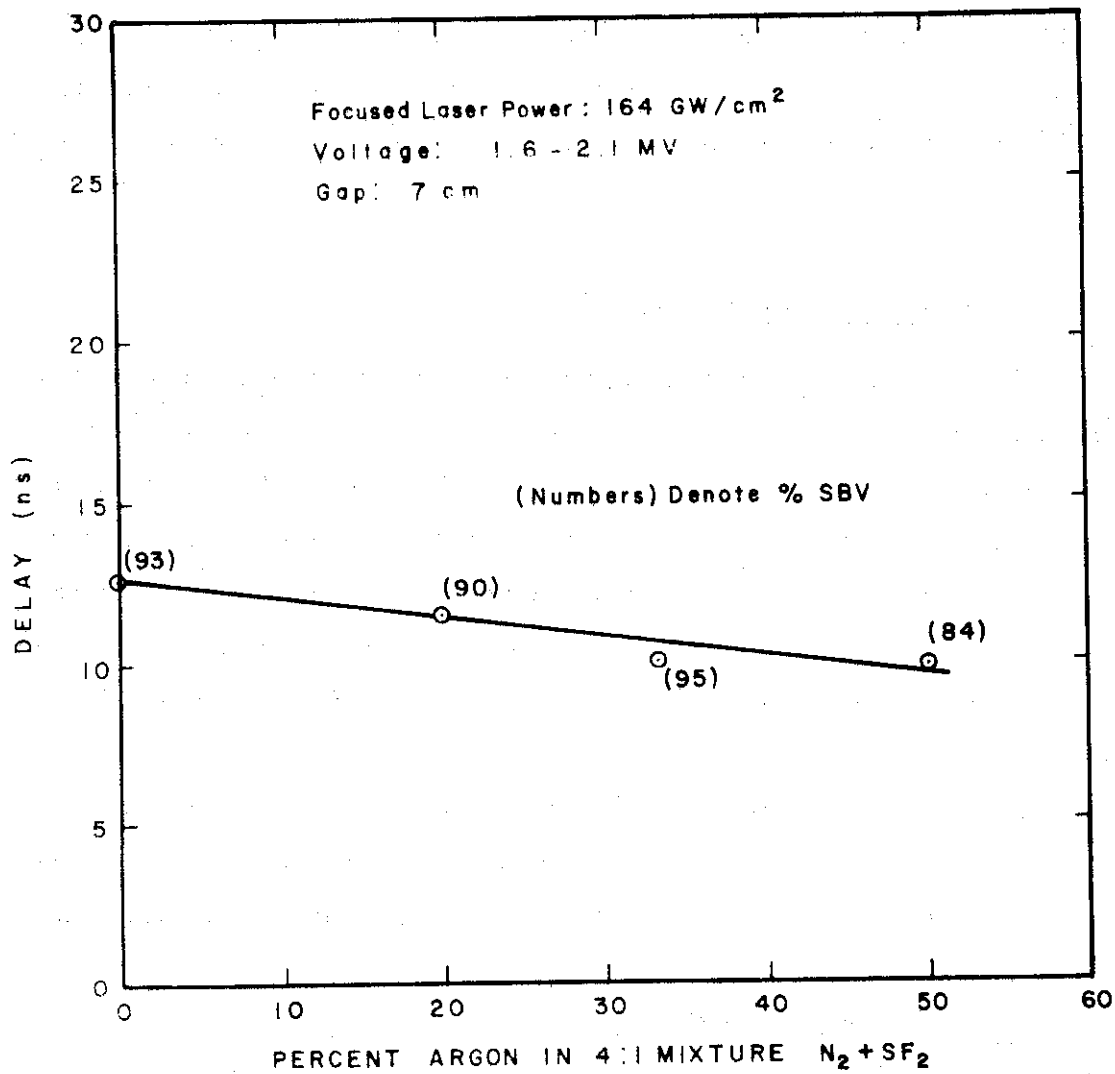


Figure 15. Delay Versus Percent Argon at 150 psig

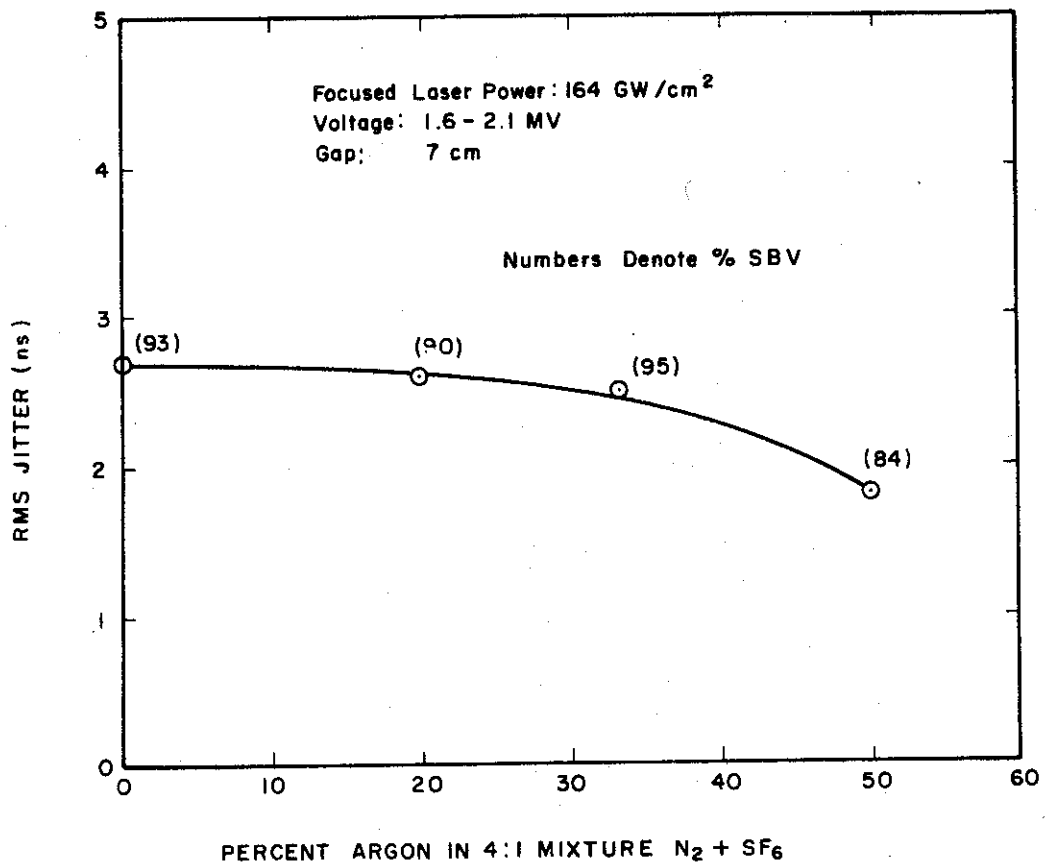


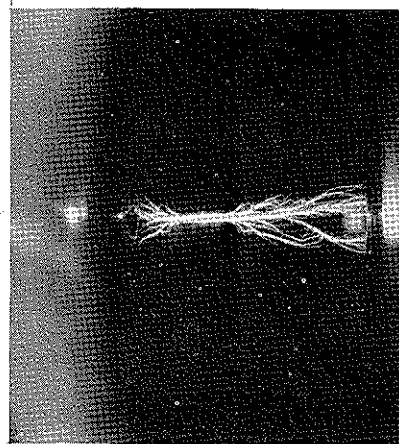
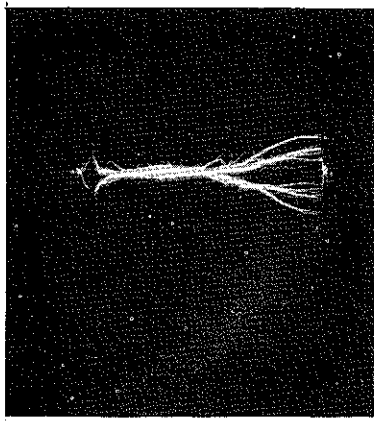
Figure 16. Jitter Versus Percent Argon at 150 psig

100% N₂

5.0% A + 40% N₂ + 10% SF₆

3.15 MV

3.06 MV



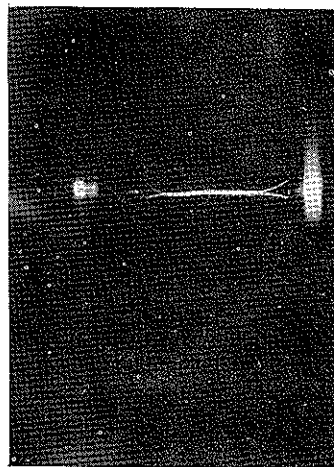
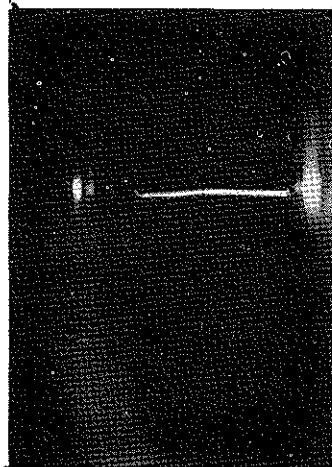
11 cm

No. 186

No. 572

2.1 MV

1.9 MV



7 cm

No. 207

No. 509

Laser Power Density 164 GW/cm²

Figure 17. Laser-Switched Discharges at 300 psig (Single Channel)

2-1300a

discharges, at operating voltages from 1.1 MV to 3.15 MV are shown in Figures 18 and 19.

Delay and risetime observed under various conditions are listed in Table 6. These data may be compared with equivalent single channel observations in Tables 2 and 3. The power density per channel was at least 80 GW/cm^2 since the higher laser power was always used. A measure of the actual laser power splitting performance during disassembly showed that 51.5% of the power went to the upper channel and 48.5% to the lower. This difference in power was attributed to a slight misalignment of the turning prism in the lower channel such that the angle of the beam at the reflecting side was not quite large enough for total internal reflection.

3.2.2 Characteristic Times for Double-Channel Switching

Five characteristic times must be considered in describing double-channel triggering:

- (1) t_g : time required for the incident laser beam to produce the initial charge carriers at the target electrode;
- (2) t_{st} : streamer transit time;
- (3) t_R : time duration of the resistive phase of the discharge defined in nanoseconds by the relation⁽¹⁴⁾

$$t_R = \frac{88}{\sqrt[3]{Z_o + Z_L (E)^{4/3}}} \left(\frac{\rho}{\rho_o} \right)^{1/2}$$

where:

- Z_o = source impedance in ohms
- Z_L = load impedance in ohms
- E = electric stress in MV/m
- ρ_o = density of air at NTP
- ρ = density of switching gas

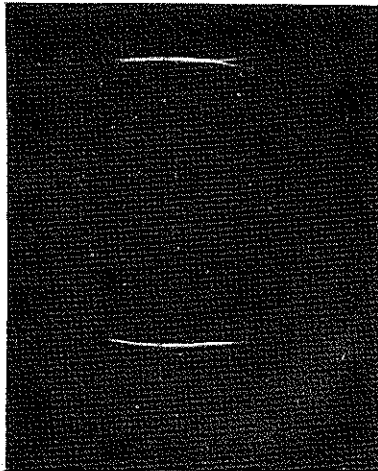
100 % N₂

50% A + 40% N₂ + 10% SF₆

1.9 MV

1.55 MV

7 cm
95% SBV



7 cm
82% SBV

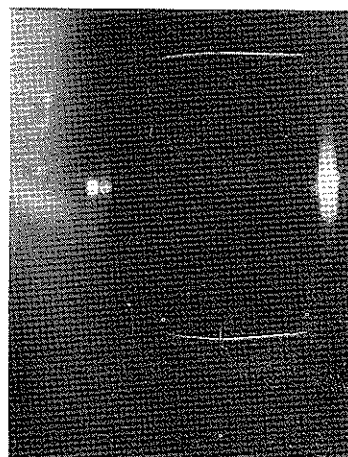
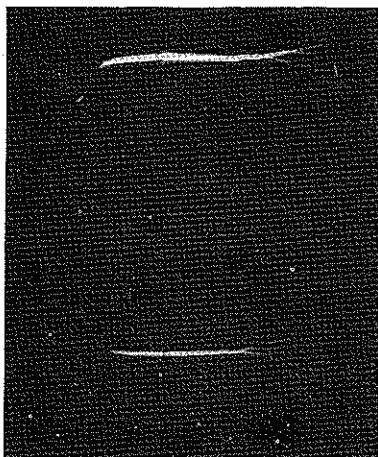
No. 22

No. 485

2.73 MV

1.1 MV

11 cm
93% SBV



7 cm
58% SBV

No. 171

No. 491

Figure 18. Laser-Switched Discharges at 150 psig
(Double Channel)

2-1301

1.9 MV

7 cm

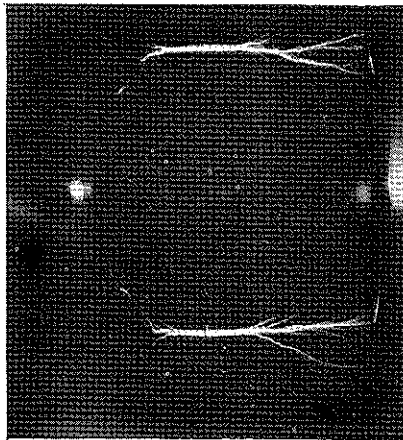


83% SBV

No. 517

3.15 MV

11 cm



97% SBV

No. 537

Figure 19.

Laser-Switched Discharges at 300 psig
(Double Channel)

2-1302

Table 6. Double-Channel Switching Results

| Gas Composition | Pressure psig | Voltage MV | Cap cm | % of SBV | E/P V/cm-torr | Number of Observations | | Delay ns | | 10 - 90% Risettime ns | |
|----------------------------|---------------|------------|--------|----------|---------------|------------------------|----------------|----------------|----------------|-----------------------|----------------|
| | | | | | | Single Channel | Double Channel | Single Channel | Double Channel | Single Channel | Double Channel |
| 100% N ₂ | 150 | -1.9 | 7 | 95 | 31.9 | 3 | 1 | 9 | 9 | 4 | 2.5 |
| | 150 | +2.73 | 11 | 93 | 29.1 | 1 | 1 | 8 | 14 | 4 | 3.5 |
| 50% A + 40% N ₂ | 150 | +1.55 | 7 | 83 | 26.0 | 6 | 1 | 12.2 ± 3.6 | 10 | 3.5 | 2.5 |
| | 150 | +1.1 | 7 | 58 | 18.5 | 9 | 4 | 17.0 ± 3.9 | 15.0 ± 2.2 | 4 | 3 |
| + 10% SF ₆ | 300 | +1.9 | 7 | 83 | 16.6 | 3 | 7 | 11.7 ± 0.6 | 11.7 ± 1.2 | 4 | 3 |
| | 300 | +3.15 | 11 | 97 | 17.6 | 2 | 6 | 19.0 ± 1.0 | 13.4 ± 1.9 | 3.5 | 3.8 |

- (4) t_L : time duration of the inductive phase of the discharge defined in nanoseconds by the relation

$$t_L = \frac{L' d}{Z_o + Z_L}$$

where:

d = gap separation

L' = channel inductance in nH per unit length

- (5) t_{sep} : separation time between triggered points on target electrode.

In order that current can be shared equally between the two channels, both channels must be initiated within the time for the gap voltage to drop significantly. The following condition⁽¹⁵⁾ expresses these limits:

$$\left| \left(t_g + t_{st} \right)_1 - \left(t_g + t_{st} \right)_2 \right| \leq t_{sep} + \left(t_R^2 + t_L^2 \right)^{1/2}$$

This expression points out the importance of using equal laser power in each channel since the formation time t_g for the two gaps must be equal. In other words, low jitter is a necessary but insufficient condition for double-channel switching; the absolute values of the times required for initial ionization and streamer passage must be equal for each channel as well. The very low jitter observed in the laser-triggered switch and the precision with which one can control laser beams make the laser especially suitable for the initiation of double-channel switches.

3. 2. 3 Risetime Considerations

The time constants of the resistive and inductive phases of switching determine the risetime of the signal transmitted to the load. These time constants may be calculated in nanoseconds from the expressions for t_R and t_L given in the previous section.

A commonly used value⁽¹⁵⁾ for channel inductance is 15 nH/cm. When two channels are used the mutual inductance between the channels must be included. The resultant switch inductance is then about 0.6 times that of the single channel. An experimental simulation of the inductance of multiple channels consisting of No. 28 wire (0.0126 inch diameter) bridging a 9 cm gap and arranged on a 20 cm diameter circle is described in Reference 12. Values of 14.2 nH/cm and 8.2 nH/cm were found for the single and double channels, respectively.

The driving impedance of FX-25 is 40 ohms per channel; the load chamber used in this experiment has an impedance of 90 ohms.

These values have been used to calculate the resistive and inductive phases for the conditions described in Table 6. The resulting 10-90% risetimes have been calculated from:

$$t_{10-90\%} = 2.2 \sqrt{t_R^2 + t_L^2}$$

The results of these calculations are presented in Table 7. Successful double-channel switching was generally more likely in the gas mixture which had a longer resistive phase than in the pure nitrogen. No attempt was made to account for the effect of multiple branching across the 11 cm gap which would further reduce t_R and t_L . The agreement between calculated and observed risetimes is closer than one would expect, considering that the measurements were made from traces with a sweep speed of 10 ns/cm. These results are encouraging and invite further study of double-channel switching with this apparatus.

Table 7. Calculated Risetimes and Time Constants

| Gas Composition | Pressure psig | Voltage MV | Gap cm | Resistive Phase ^{ns} | | Inductive Phase ^{ns} | | Risetime, 10%-90% ^{ns} | |
|--|---------------|------------|--------|-------------------------------|----------------|-------------------------------|----------------|---------------------------------|----------------|
| | | | | Single Channel | Double Channel | Single Channel | Double Channel | Single Channel | Double Channel |
| 100% N ₂ | 150 | -1.9 | 7 | 0.66 | 0.60 | 1.78 | 1.07 | 2.3 | 1.7 |
| | 150 | +2.73 | 11 | 0.75 | 0.69 | 2.79 | 1.68 | 3.2 | 2.3 |
| 50% A + 40% N ₂ + 10% SF ₆ | 150 | +1.55 | 7 | 1.12 | 1.03 | 1.78 | 1.07 | 3.1 | 2.5 |
| | 150 | +1.1 | 7 | 1.84 | 1.68 | 1.78 | 1.07 | 4.4 | 3.8 |
| | 300 | +1.9 | 7 | 1.20 | 1.10 | 1.78 | 1.07 | 3.2 | 2.6 |
| | 300 | +3.15 | 11 | 1.133 | 1.04 | 2.79 | 1.68 | 3.7 | 2.8 |

This page intentionally left blank.

SECTION 4

COMPLEMENTARY RESULTS FROM SIEGE II PROGRAM

During the recent study of the SIEGE II system⁽⁴⁾ it was necessary to simulate the operating environment by extending the effective path between laser and switch to greater than 20 m by passing the beam through an array of six 90-degree turning prisms. A diagram of this experiment is shown in Figure 20. Photographs of the apparatus in the FX-25 area are shown in Figures 21 and 22. The simplicity and vulnerability to misalignment of this arrangement are obvious.

Despite a setup which would be considered crude by optical engineering standards, our switching results are quite encouraging. Histograms of delay measurements are shown for both a positive and a negative terminal in Figures 23 and 24. The delays are 67.6 ± 1.8 ns for a positive terminal fired by 100 MW of laser power and 60.2 ± 1.0 ns for a negative terminal fired by 125 MW of laser power.

A photograph of one of the discharges observed in nitrogen switched by laser 20 m away was shown earlier in Figure 9. A sample of the delay data was shown in Figure 10. The measurements from these traces, after correction for laser time-of-flight and cable length differences, are shown together with many other measurements in Figure 23.

The spot size at the target was calculated from Kogelnik's⁽⁵⁾ analysis to have an area of 1.82×10^{-3} cm². This yielded power densities of 54.5 and 68.2 GW/cm² for the 100 and 125 MW levels, respectively, at the Elkonite target. The laser powers quoted are those incident on the target electrode. Note that the higher power density gave shorter delay and jitter and was essentially equal to the 65 GW/cm² level used in the earlier work, whereas the lower power density was 16% lower than that used earlier.

It is interesting to compare the results at approximately 2-meters and 20-meters separation. Both the power density and jitter have remained constant, but the delay has increased an order of magnitude. The only other

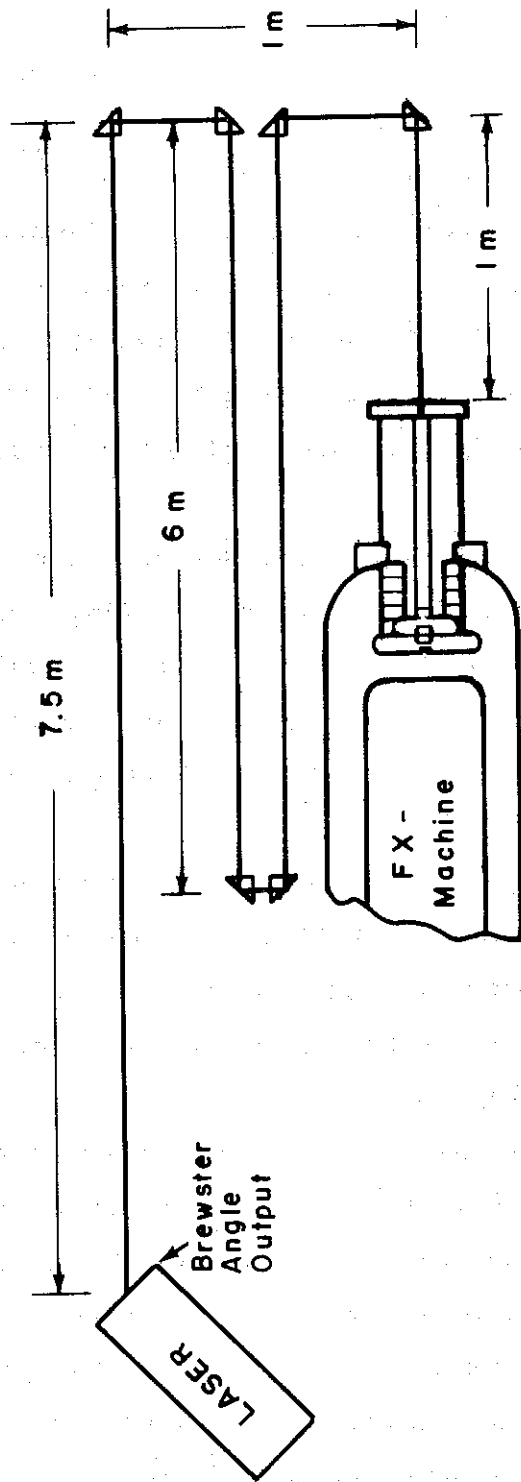
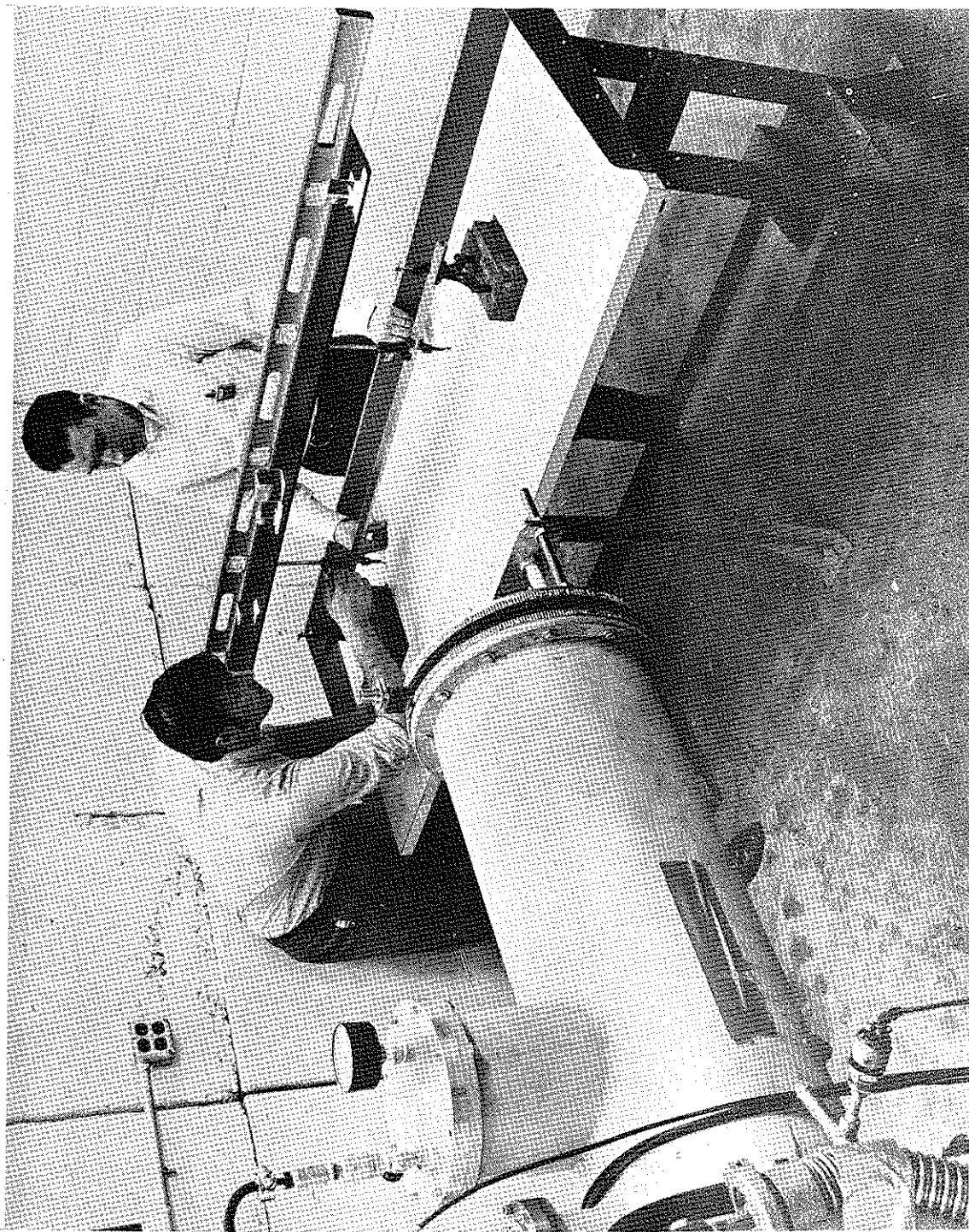


Figure 20. Diagram of Laser Triggering at 20 m



2-1262

Figure 21. Laser-Switch Load Assembly and Turning Prisms

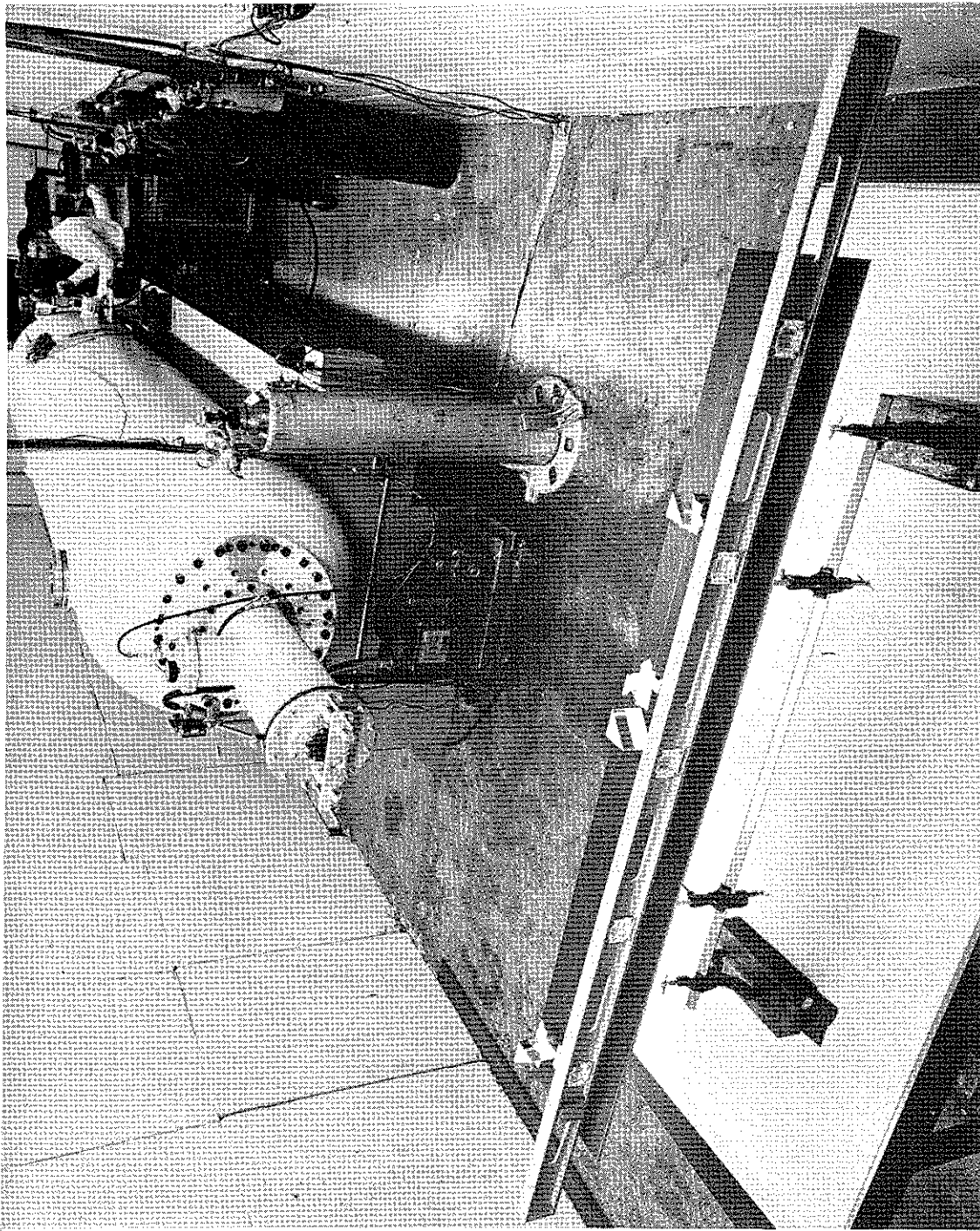
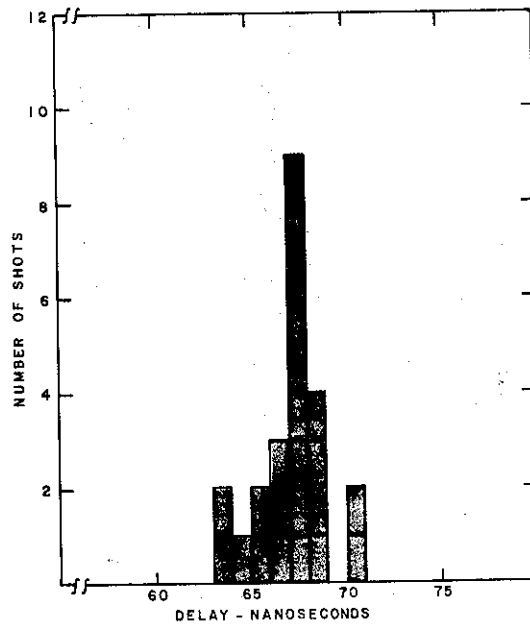


Figure 22. Apparatus for Laser-Triggering 2-MV
Switch Over 20-Meter Path

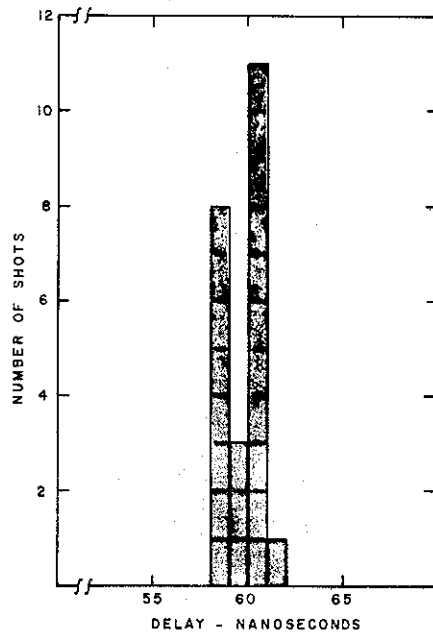
2-1263



Gas: 150 psig, 100% N₂
 Gap: 7 cm
 Terminal: +1.55 MV, 83% SBV
 Laser: 100 MW
 Distance: 22 m
 Delay: 67.6 ± 1.8 ns

Figure 23. Switch Delay in N₂ at 22 m
(100 MW Laser)

1-3638



Gas: 150 psig, 100% N₂
 Gap: 7 cm
 Terminal: -1.55 MV, 83% SBV
 Laser: 125 MW
 Distance: 22 m
 Delay: 60.2 ± 1.0 ns

Figure 24. Switch Delay in N₂ at 22 m (125 MW Laser)

factor that appears significant is the larger beam diameter entering the focusing lens in the 20-meter case. The diameter in the latter case is at least twice that of the 2-meter work. Hence, the focusing cone angle is also greater in the gap. This could result in less effective pre-ionization of the gap because of the reduced power density away from the target.

A rough check on this behavior was made by reducing the effective laser-to-gap path length to 10 meters in order to reduce the beam diameter entering the lens and the focusing cone angle in the gap. This was accomplished by removing the middle four turning prisms from the path shown in Figure 20. As predicted, the delay observed had a value between that for the 2-meter and 20-meter experiments, and the jitter remained constant. In this case, however, the power density calculated at the target was approximately double that at 20 meters, even though the input power remained constant. A summary and comparison of these observations with the 2-meter case are given in Table 8.

A possibility existed that the variation of the position of minimum beam waist in the gap, calculated from Equation (A-3) of the Appendix, contributed to longer switching delay observed at greater laser-to-lens distance. This was briefly investigated by moving the focusing lens approximately 1-cm closer to the target when the laser was 20 meters away from switch assembly. This lens position placed the minimum waist at approximately the same point as it was when the laser was only 2 meters away. The discharge patterns observed were very poor, and switch operation was unpredictable. It was concluded that the variation in the position of minimum beam waist could not explain the observed long delays and low jitter.

Although a great deal more study and experimentation is needed to adequately explain these results, some observations of Basov⁽¹⁶⁾ and his co-workers may provide some insight. This group examined the influence of laser beam-focusing on air breakdown by varying the focal length of their lenses. When operating their Q-switched neodymium laser in 130-MW pulses of 15-ns (FWHM) duration, they measured the longitudinal movement of the spark traveling toward the lens as a function of time. The velocity of this motion

Table 8. Effect of Laser-to-Switch Separation
(Nitrogen at 150 psig)

| Separation (m) | Voltage (MV) | Gap (cm) | Percent of SBV | Number of Measurements | Delay (ns) | Jitter (ns) | Laser Power Density (GW/cm ²) |
|-------------------|-----------------|-------------|-------------------|---------------------------|---------------|----------------|--|
| 2 | -1.9 | 7 | 95 | 16 | 6.2 | ±1.4 | 65 |
| 2 | +1.05 | 7 | 50 | 23 | 14.3 | ±1.6 | 65 |
| 10 | -1.55 | 7 | 83 | 22 | 21.0 | ±1.2 | 130 |
| 20 | -1.55 | 7 | 83 | 23 | 60.2 | ±1.0 | 68 |

during the first 10 ns increased from a value of 2.4×10^7 cm/sec to 9×10^7 cm/sec when the focal length of the lens was changed from 4 cm to 20 cm. In other words, the spark traveled faster when the cone angle was smaller, since the beam diameter at the lens remained constant.

This page intentionally left blank.

SECTION 5 CONCLUSIONS

The primary objective of this study, to extend laser-triggered switching technology into the multimegavolt region, has been realized. Both single- and double-channel laser switching have been examined in the range from 1 MV to more than 3 MV. Jitter times of the order of 1 to 3 ns were observed in many cases.

Some questions concerning the effect of cone angle of the laser radiation crossing the gap have been raised. This factor, and, consequently the lens focal length, may be of more significance in the higher voltage regions where the gap distance is necessarily large. The longer delays observed when the cone angle was enlarged are consistent with the variation in spark velocity with focal length observed in Basov's experiment.⁽¹⁶⁾

Double-channel triggering was found to significantly improve rise-time in some cases. Additional work on this application with even more precise power splitting would further demonstrate the advantages of this mode of switching and provide worthwhile design information.

It would be very desirable to examine in detail the phenomena which occur at or near the target in order to establish the most efficient design criteria.

The most advantageous aspects of laser triggered switching from the system engineering viewpoint are its low jitter and built-in voltage isolation. The command jitter of the Q-switched laser itself has recently been demonstrated⁽¹⁷⁾ to be within ± 1 ns. The experimental work described in this report has resulted in the design of laser-triggered switches operated at more than 3 MV within a jitter time of less than ± 1 ns.

These features of the laser and the laser-triggered switch make feasible the design of multimegavolt pulse generators with tight

specifications on either series or parallel synchronization. Such applications may require either the simultaneous switching of several energy stores into a load, or the sequential firing of several switches, as in a sophisticated Marx generator or a phased array of electromagnetic pulse generators.

SECTION 7
REFERENCES

1. Pendleton, W. K. and Guenther, A. H. , "Investigation of a Laser-Triggered Spark Gap", Rev. Sci., Inst. 36, 1546 (1965)
2. Guenther, A. H. and McKnight, R. H. , "A Laser-Triggered 50 pps High-Voltage Switch with Nanosecond Jitter", Proc. IEEE 55, 1504 (1967).
3. Guenther, A. H. and Bettis, J. R. , "Laser-Triggered Megavolt Switching", IEEE J. of Quantum Electronics, QE-3, 581 (1967)
4. "SIEGE II, Phase II", Technical Report No. AFWL-TR-69-81, Volume III, p. 3-146 (June 1969)
5. Kogelnik, H. , "Imaging of Optical Modes-Resonators with Internal Lenses", BSTJ 44, 455 (1965)
6. Bruce, C. W. and Collet, E. H. , "Pulse Laser Instrumentation", Technical Report No. WL-TR-64-127, p. 27 (June 1965)
7. Laser-Triggered Switching Study, Monthly Progress Letter No. 3, submitted by IPC to AFWL under Contract F29601-69-C-0001 (January 1969)
8. Mack, C. , Essentials of Statistics, Plenum Press (1967) pp. 35 and 70.
9. Winer, I. M. , "A Self-Calibrating Technique Measuring Laser Beam Intensity Distributions", Applied Optics 5, 1437 (1966)
10. Brode, R. B. , "The Quantitative Study of Collisions of Electrons with Atoms", Rev. Mod Phys. 5, 257 (1933)
11. Francis, G. , Ionization Phenomena in Gases, Academic Press p. 31 (1960)

12. Brown, S. C., Basic Data of Plasma Physics, 1966 M. I. T. Press (1967) 2nd ed., p. 143
13. Guenther, A. H., "Recent Developments in Laser-Triggered Switching", DASA Information and Analysis Center, Dasiac Special Report No. 80, p. 48 (April 1968)
14. Martin, J. C., "Duration of the Resistive Phase and Inductance of Spark Channels", AWRE Internal Report SSWA/JCM/1065/25
15. Electromagnetic Pulse System Study Ares I, Phase I, Final Report submitted under EG&G subcontract No. A-2743, Volume II, Section A. 5. 4
16. Basov, N. G., Boiko, V. A., Krokhin, O. N., and Sklizkov, G. V., "Influence of Laser Radiation Focusing on the Air Breakdown", Proc. 8th International Conf. on Phenomena in Ionized Gases, (Vienna, Austria) International Atomic Energy Agency, 1967, p. 261
17. Hardway, G. A., Guenther, A. H. and Graf, A. K., "Applications of High Power Lasers", submitted to Proceedings of New York Academy of Sciences and summarized in Laser Focus, p. 25 (June 1969)

APPENDIX

CALCULATION OF POWER DENSITY AT TARGET ELECTRODE

The spot size at the target electrode varies with the laser beam divergence, focal length of focusing lens, wavelength, and laser to lens distance according to Kogelnik's⁽⁵⁾ analysis of Gaussian beams.

These variables are defined in Figure A-1. The value of the beam waist w_1 is given from

$$\theta_1 = \frac{2\lambda}{\pi w_1} \quad (\text{A-1})$$

where θ_1 is the full-angle beam divergence. The distance d_1 can be estimated by finding the position of w_1 on a cone having an apex angle θ_1 and an exit face equal to the amplifier rod. The radius of the minimum focal spot is then given by

$$\frac{1}{w_2^2} = \frac{1}{w_1^2} \left(1 - \frac{d_1}{f} \right)^2 + \frac{1}{f^2} \left(\frac{\pi w_1^2}{\lambda} \right)^2 \quad (\text{A-2})$$

where f is the focal length of the lens and λ is the laser radiating wavelength. The position of this minimum is given by

$$d_2 - f = (d_1 - f) \frac{f^2}{(d_1 - f)^2 + \left(\frac{\pi w_1^2}{\lambda} \right)^2} \quad (\text{A-3})$$

In the cases of interest to this study, the target was placed 1.5 mm closer to the lens than f . Therefore, the spot size at the target was obtained from

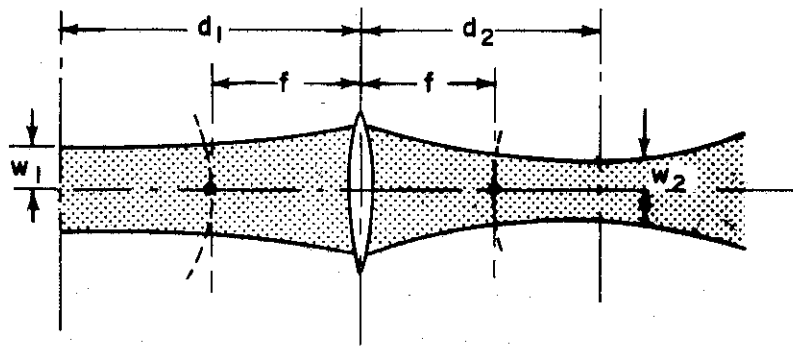


Figure A-1. Gaussian Beam Transformed by a Lens

$$[w(z)]_{\text{target}}^2 = w_2^2 \left[1 + \left(\frac{\lambda z}{\pi w_2^2} \right)^2 \right] \quad (\text{A-4})$$

$$z = d_2 - f + 1.5 \text{ mm} \quad (\text{A-5})$$

The full-angle beam divergence as a function of laser output power is shown in Figure A-2. Two values of flashlamp supply capacitance gave slightly different divergence at the same power level. Since the lower capacitance was used in the 100-MW level experiments, the corresponding beam divergence was chosen for spot size calculation.

A further complication is the fact that the output from the Brewster angle amplifier is elliptical and results in a vertical and horizontal beam divergence of substantial difference. The horizontal value is greater because the beam undergoes refraction in that plane. A separate value of beam waist was calculated for the vertical and horizontal planes and an elliptical spot was assumed in calculating the area of the spot at the cathode. The laser power density incident at the target was then determined for the power levels and laser-to-gap separations used in the experiment. The results of these calculations are listed in Table A-1.

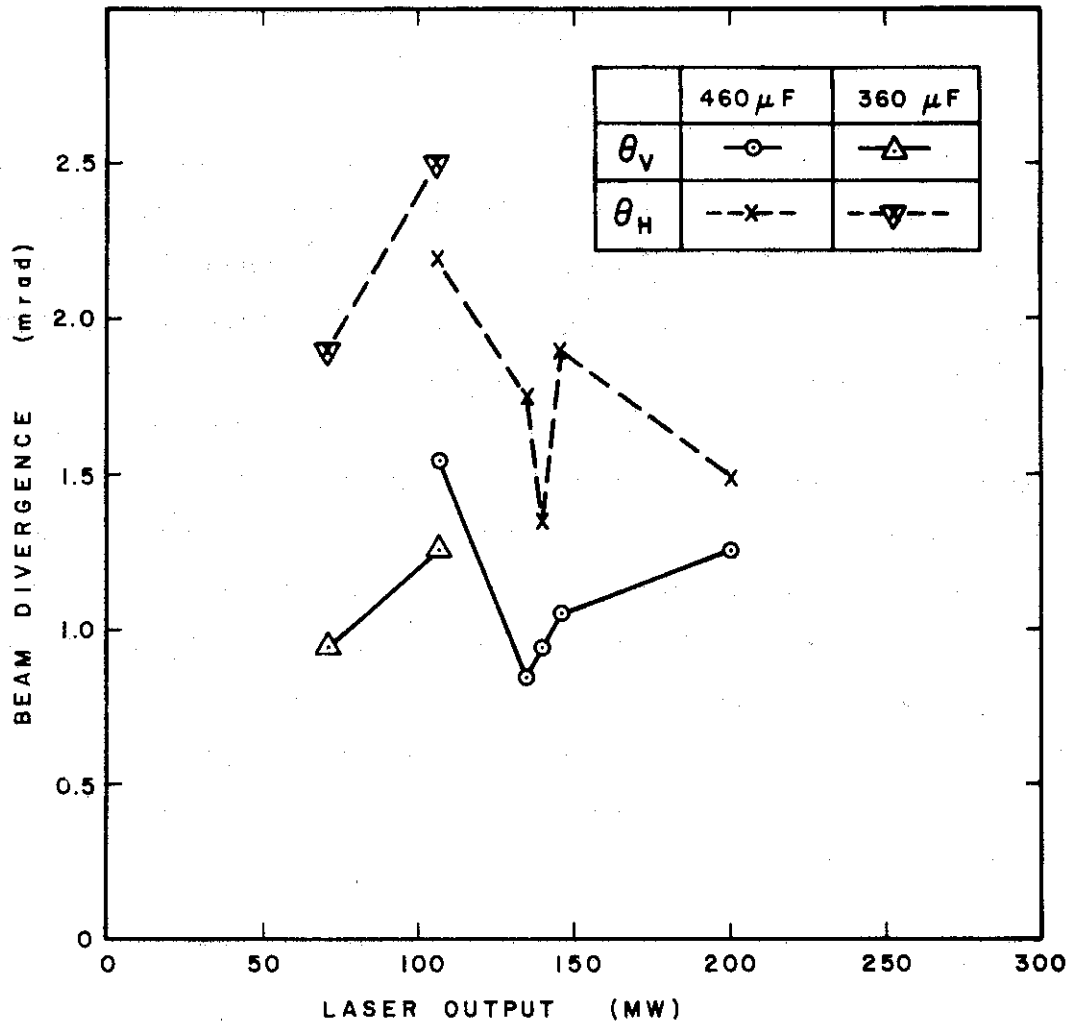


Figure A-2. Beam Divergence of K-1500 Laser System

Table A-1. Power Densities at Target

| Laser Output MW | θ_V mrad | θ_H mrad | Laser To Gap Meters | R_V cm | R_H cm | Spot Area cm^2 | Power Into Gap MW | Power Density At Target GW/cm^2 |
|-----------------|-----------------|-----------------|---------------------|-----------------------|-----------------------|-------------------------|-------------------|---|
| 100 | 1.25 | 2.5 | 2 | 1.72×10^{-2} | 2.42×10^{-2} | 13.1×10^{-4} | 85 | 65 |
| 200 | 1.25 | 1.5 | 2 | 1.72×10^{-2} | 1.81×10^{-2} | 9.75×10^{-4} | 160 | 164 |
| 200 | 1.25 | 1.5 | 10 | 1.6×10^{-2} | 1.91×10^{-2} | 9.6×10^{-4} | 125 | 130 |
| 200 | 1.25 | 1.5 | 20 | 2.21×10^{-2} | 2.64×10^{-2} | 18.4×10^{-4} | 100 | 54 |
| 200 | 1.25 | 1.5 | 20 | 2.21×10^{-2} | 2.64×10^{-2} | 18.4×10^{-4} | 125 | 68 |

DISTRIBUTION

No. cys

HEADQUARTERS USAF

Hq USAF, Wash, DC 20330

1 (AFCSAMI)
 1 (AFOCELA)
 2 (AFRDQSN, 1D425)
 1 (AFRDQSS)
 1 USAFCEC (CEC-E), Wright-Patterson AFB, OH 45433
 2 USAF Dir Nuc Safety (AFINS), Kirtland AFB, NM 87117

MAJOR AIR COMMANDS

AFSC, Andrews AFB, Wash, DC 20331

1 (SCOC)
 4 (SCSE)
 2 (SCT)
 1 (SCTS)
 1 (SCTSE)
 2 (SCTSW)
 1 AUL (SE)-67-464, Maxwell AFB, AL 36112
 1 AFIT Lib, Bldg 640, Area B, Wright-Patterson AFB, OH 45433
 USAF Academy, CO 80840
 1 (DFSLB)
 1 (DFSFR)

AFSC ORGANIZATIONS

1 FTD (TDBID), Wright-Patterson AFB, OH 45433
 1 ARL (STINFO, ARIR, R. C. Cook), Wright-Patterson AFB, OH 45433
 1 AFAL, Wright-Patterson AFB, OH 45433
 1 Comdr, OAR (RRRD), Holloman AFB, NM 88330
 LAAFA, SAMSO, AFUPO, Los Angeles, CA 90045
 2 (AFL 2822/SMMPP-4)
 1 (SMT)
 1 (SMTG)
 1 (SMTC)
 1 (SMTN)
 SAMSO, Norton AFB, CA 92409
 1 (SMQNM)
 1 (SMY)
 1 (SMYSE)

DISTRIBUTION (cont'd)

No. cys

2 ESD (ESTI), L. G. Hanscom Fld, Bedford, MA 01730
 4 RADC (EMTLD), Griffiss AFB, NY 13440
 1 AFRPL (RPRR), Edwards AFB, CA 93523

KIRTLAND AFB ORGANIZATIONS

AFSWC, Kirtland AFB, NM 87117
 1 (SWEH)
 1 (SWF)
 1 (SWV)
 1 (SWVT, Dr. David Dye)
 AFWL, Kirtland AFB, NM 87117
 12 (WLOL)
 1 (WLC)
 1 (WLE)
 2 (WLR)
 150 (WLRE, Capt Baum)
 1 (WLT)
 14 (WLZS)
 1 (WLX)

OTHER AIR FORCE AGENCIES

1 Dir, USAF Proj RAND, via: AFLO, RAND Corp (Dr. Karzas), 1700 Main St, Santa Monica, CA 90401

ARMY ACTIVITIES

Comdg Off, Diamond Lab, Wash, DC 20438
 1 (Mr. Caldwell, Tech Lib)
 1 (Mr. Oswald)
 2 Dept of Army NIKE-X Fld Ofc (AMCPM-NXE-FB), Bell Tel Lab, Whippany, NJ 07981
 Comdg Gen, Redstone Arsenal, AL 35809
 1 (Maj Ogden, USA Safe Sys Comd, P. O. Box 1500)
 1 (Dr. Roberts, Sci Info Cen, USA Msl Comd)
 1 Comdg Off, Ballistic Rsch Lab (Mr. Edward Bryant), Aberdeen Proving Gnd, MD 21005
 Comdg Off, Picatinny Arsenal, Dover, NJ 07801
 4 (SMUPA-VCl)
 1 (Mr. Louis Avrami)
 1 Comdg Gen, USA Mat Comd (AMCRD-BN-RE, Mr. Corrigan), Wash, DC 20315

DISTRIBUTION (cont'd)

No. cys

2 Dir, NSA (C31), Ft Meade, MD 20755
 1 Dir, USA Nuc Def Lab (Tech Lib), Edgewood Arsenal, MD 21010

NAVY ACTIVITIES

Dir, NRL, Wash, DC 20390
 2 (Code 2027)
 1 (Dr. Kolb)
 1 (Mr. DePackh)
 1 (Dr. Lupton)
 1 (Mr. Vitkovitzky)
 1 (Dr. Levine)
 2 Comdg Off, Nuc Wpns Tng Cen (Nuc War Dept), Atl, NAS, Norfolk, VA 23511
 1 Comdr, NWC (Code 753), China Lake, CA 93557
 1 Comdr, NOL (Code 730), White Oak, Silver Spring, MD 20910
 1 Dir, Spec Proj Ofc, Dept Navy, Wash, DC 20360
 2 Comdg Off, NWEF (Code ADS), Kirtland AFB, NM 87117

OTHER DOD ACTIVITIES

Dir, DASA, Wash, DC 20305
 1 (Tech Lib)
 1 (SPSS)
 Dir, ARPA, DOD, Pentagon, Wash, DC 20301
 1 (Tech Lib)
 1 (Dr. J. Wade)
 20 DDC (TCA), Cameron Sta, Alexandria, VA 22314

AEC ACTIVITIES

USAEC, Rm J-004, Wash, DC 20545
 1 (Asst Gen Mgr, Mil Appl)
 2 (Div Rsch, Dr. B. Eastlund and Dr. R. Hirsch)
 Sandia Corp, Box 5800, Sandia Base, NM 87115
 2 (Info Dist Div)
 1 (Dr. Bechner)
 1 (A. W. Snyder)
 1 (Mr. Martin)
 Sandia Corp, P. O. Box 969, Livermore, CA 94550
 1 (Org 8000, Dr. T. Cook)
 1 (Dr. Rohwein)

DISTRIBUTION (cont'd)

No. cys

| | |
|---|--|
| 1 | USAEC, Div Tech Info Ext (Doc Mgt Br), P. O. Box 62, Oak Ridge, TN 37830 |
| 1 | UCLRL (Tech Info Div), Berkeley, CA 94720 Dir, LASL, P. O. Box 1663, Los Alamos, NM 87554 |
| 1 | (Rpt Lib) |
| 1 | (Dr. Mather) |
| | OTHER |
| 1 | Admin Gp on Elec Devices (Daniel Kleger), 201 Varich St, 9th Floor, New York, NY 10014 |
| | Aerospace Corp, SB Ops, P. O. Box 1308, San Bernardino, CA 92402 |
| 1 | (Tech Lib) |
| 1 | (Dr. Josephson) |
| 1 | Bell Tel Lab (Tech Rpt), Rm 2A165B, Whippany, NJ 07981 |
| 1 | Clearinghouse (410.11), 5285 Port Royal Rd, Springfield, VA 22151 |
| | Cornell Univ, Ithaca, NY 14850 |
| 1 | (Prof N. Rostoker) |
| 1 | (Prof S. Linke) |
| 1 | (Prof H. Fleischman) |
| 1 | (Dr. M. Andrews) |
| 1 | (Prof J. Nation) |
| 1 | EG&G (Mr. Kramer), P. O. Box 227, Bedford, MA 01730 |
| 1 | GE Co-MSD (L. I. Chasen, Lib), Philadelphia, PA 19101 |
| 1 | Gulf Gen Atomic Inc (Lib), P. O. Box 608, San Diego, CA 92112 |
| | Ion Phys Corp, South Bedford St, Burlington, MA 01803 |
| 1 | (Dr. Nablo) |
| 1 | (Dr. Uglam) |
| 1 | (Mr. Graybill) |
| 1 | (Mr. Cheever) |
| 1 | Kaman Nuc (Dr. A. P. Bridges), 1700 Garden of the Gods Rd, Colorado Springs, CO 80907 |
| 1 | MIT (Lincoln Lab, Doc Lib), P. O. Box 73, Lexington, MA 02173 |
| | Maxwell Lab, Inc, 9244 Balboa Ave, San Diego, CA 92123 |
| 1 | (Mr. Crewson) |
| 1 | (Mr. Fitch) |
| 1 | (Dr. O'Rourke) |
| 1 | (Mr. Jones) |

DISTRIBUTION (cont'd)

No. cys

- 1 NASA Manned Spcft Cen (Chief, Tech Info Div), Houston, TX 77001
- 1 NASA Sci & Tech Info Fclty (Acquis Br, S-AK/DL), P. O. Box 33,
College Park, MD 20740
Phys Internat, 2700 Merced St, San Leandro, CA 94577
- 1 (Dr. Yonas)
- 1 (Mr. Smith)
- 1 TRW Sys Gp (Tech Lib, Doc Acquis), 1 Space Park, Redondo Beach, CA
90276
- 1 Varian Assoc, Cen Rsch Lab (Dr. Jory), 611 Hansen Way, Palo Alto, CA
94304
- 1 Westinghouse Elec Corp, Elec Tube Div (Shelden S. King, Tech Info),
Box 284, Elmira, NY 14902
- 1 Official Record Copy (Capt Bettis, WLZS)

UNCLASSIFIED

Security Classification

DOCUMENT CONTROL DATA - R & D

(Security classification of title, body of abstract and indexing annotation must be entered when the overall report is classified)

| | | | |
|---|------------------|---|-----------------|
| 1. ORIGINATING ACTIVITY (Corporate author) | | 2a. REPORT SECURITY CLASSIFICATION | |
| Ion Physics Corporation Burlington, Massachusetts 01803 | | UNCLASSIFIED | |
| | | 2b. GROUP | |
| 3. REPORT TITLE | | | |
| LASER-TRIGGERED SWITCHING STUDY | | | |
| 4. DESCRIPTIVE NOTES (Type of report and inclusive dates) | | | |
| September 1968-May 1969 | | | |
| 5. AUTHOR(S) (First name, middle initial, last name) | | | |
| John J. Moriarty | | | |
| 6. REPORT DATE | | 7a. TOTAL NO. OF PAGES | 7b. NO. OF REFS |
| December 1969 | | 72 | 17 |
| 8a. CONTRACT OR GRANT NO. | F29601-69-C-0001 | 9a. ORIGINATOR'S REPORT NUMBER(S) | |
| b. PROJECT NO. | 5710 | AFWL-TR-69-87 | |
| c. Subtask No. | RRL 1053 | 9b. OTHER REPORT NO(S) (Any other numbers that may be assigned this report) | |
| d. | | | |
| 10. DISTRIBUTION STATEMENT | | | |
| This document has been approved for public release and sale; its distribution is unlimited. | | | |
| 11. SUPPLEMENTARY NOTES | | 12. SPONSORING MILITARY ACTIVITY | |
| | | AFWL (WLZS) Kirtland AFB, NM 87117 | |
| 13. ABSTRACT | | | |
| (Distribution Limitation Statement No. 1) | | | |
| Single- and double-channel laser-triggered switches in high-pressure gas have been designed and operated in the voltage range from 1 MV to more than 3 MV. Jitter times of 1 to 3 ns were observed in most cases. Gas pressures of 150 psig and 300 psig were used. The gases were 100 percent nitrogen and a 4:1 mixture (by partial pressure of N ₂ + SF ₆ enriched with up to 50 percent argon. Significant accomplishments were (1) the simultaneous firing of four stages of a Marx generator by a multiply split laser-beam; (2) up to 40 percent reduction in the risetime observed in the output pulse from a multimegavolt dc generator when switched into a load through two simultaneously laser-triggered channels; and (3) the design and operation of a laser-triggered, dc-charged switch at more than 3 MV with subnanosecond jitter. | | | |

DD FORM 1 NOV 65 1473

UNCLASSIFIED

Security Classification

| 14. KEY WORDS | LINK A | | LINK B | | LINK C | |
|---|--------|----|--------|----|--------|----|
| | ROLE | WT | ROLE | WT | ROLE | WT |
| Laser-triggered switching Spark-gap conduction Nanosecond timing Laser-surface interactions Dielectric conduction Plasma switch High-voltage switch Multiple-channel switch Multiple-gap switch | | | | | | |